T H E U N I V E R S I T Y O F A L B E R T A

RELEASE FORM

NAME OF AUTHOR: Santosh S. Sikerwar

TITLE OF THESIS: Studies on the Sub-unit Structure of the Inner Mitochondrial Membrane

DEGREE FOR WHICH THESIS WAS PRESENTED: M.Sc.

YEAR THIS DEGREE GRANTED: 1978

THE UNIVERSITY OF ALBERTA

STUDIES ON THE SUB-UNIT STRUCTURE OF THE INNER MITOCHONDRIAL MEMBRANE

by

© SANTOSH S. SIKERWAR

A THESIS

SUBMITTED TO THE FACULTY OF GRADUATE STUDIES AND RESEARCH

IN PARTIAL FULFILMENT OF THE REQUIREMENTS FOR THE DEGREE OF

Master of Science

in

Cell Biology

DEPARTMENT OF ZOOLOGY

EDMONTON, ALBERTA

SPRING 1978

THE UNIVERSITY OF ALBERTA

FACULTY OF GRADUATE STUDIES AND RESEARCH

The undersigned certify that they have read, and recommend to the Faculty of Graduate Studies and Research, for acceptance, a thesis entitled, "Studies on the Sub-unit Structure of the Inner Mitochondrial Membrane" submitted by Santosh S. Sikerwar in partial fulfilment of the requirements for the degree of Master of Science in Cell Biology.

Dedicated to my parents

and my brother

ABSTRACT

Structural organization of the inner mitochondrial membrane, isolated in the form of the inside-out vesicles called the sub-mitochondrial particles (SMP), has been investigated in the present work. The appearance of F_1-ATPase molecules in the negatively stained preparations of isolated mitochondrial membrane has led many workers to suggest that there is a regularly repeating structure in the inner mitochondrial membrane. In the present work experiments have been carried out to explore the periodic two-dimensional structure within the plane of inner mitochondrial membrane in SMP. SMP prepared from beef heart mitochondria have been negatively stained with 2% PTA (pH 7.1), and subsequently photographed in an electron microscope suitably modified to reduce the specimen damage due to the electron beam. To enhance the high resolution components in the image, the electron micrographs were taken at underfocus settings. Such micrographs of negatively stained SMP have been subjected to the optical diffraction analysis, and the resulting optical Fourier transforms have revealed an absence of any periodic two-dimensional structure within the plane of the membrane, thereby negating the possibility of a sub-unit structure in the membrane as discerned in SMP.

Spatial arrangement of the intramembranous proteins in the hydrophobic interior of the membrane has been examined by freeze-etching of the SMP preparations suspended in glycerol or water. This technique provides the direct visualization of membrane proteins present both on the surface and in the hydrophobic zone of the membrane. The concave (PF) and convex (EF) fracture faces display the presence of typical intramembranous particles ranging in diameter from 4nm to 16nm. An asymmetry in the distribution of these particles between the two fracture faces has been noted. The packing density of particles in the concave fracture face (PF) is 2000 ± 200 particles/μm^2 and in the convex fracture face (EF) is 1300 ± 300 particles/μm^2. Most of the particles fall into the size range 10-12nm, followed by 5-7nm range. On comparing the frequency distribution of particle sizes with frequency distribution of the sizes of the members of respiratory chain calculated from the available data, it can be inferred that there is no direct correspondence between the intramembranous particles and individual members of respiratory chain. It appears therefore that the components of respiratory chain are involved in molecular associations, which may occur between members of the respiratory chain. Such associations would be distinctly advantageous as they may facilitate cooperative interactions.

The optical diffraction experiments on the electron micrographs of freeze-fracture replicas display

a diffuse ring extending from about 9 to 12nm in the optical Fourier transforms. Had there been a regular two-dimensional lattice of intramembranous particles in the hydrophobic interior of the membrane of SMP, the optical Fourier transforms should have displayed sharp diffraction spots or ring(s). Therefore, it appears that there is a lack of any regular two-dimensional periodic arrangement of the particles in the hydrophobic interior of the membrane of SMP. This may reflect the fluid matrix of the membrane, as most biological membranes are currently thought to have.

An attempt has also been made to visualize the F_1-ATPase knobs on the surface of SMP by freeze-etching SMP suspended in water. The resulting freeze-etch replicas have revealed a smooth etched surface (PS). This observation is contradictory to what is expected on the basis of negative staining experiments on SMP which have displayed the presence of ~10nm F_1-ATPase knobs attached to the surface of SMP by the stalks. Consequently the in vivo organization of F_1-ATPase particles in relation to the rest of the membrane remains uncertain.

ACKNOWLEDGEMENT

I am extremely indebted to Prof. S. K. Malhotra for bringing me into the exciting field of membrane biology. It was he who first had me introduced to the "purple membrane" and without this I could not have "better" appreciated the role played and to be played by electron microscopy in the membrane research. His guidance, encouragement and patience were a great help during the completion of this work.

I would also like to thank Prof. S. Sheinin for some very helpful discussions and suggestions. I also thank Dr. D. Scraba for generously extending his facility of optical diffractometer.

I acknowledge the members of my committee for reading the thesis.

I wish to thank Dr. Mike Tu for being my mentor in the freeze-etch technique and for lending an astute ear to my interpretations.

I would also like to thank Mr. Harold Batz for his excellent technical assistance and for keeping the Philips EM300 ready for my regular nocturnal encounters with it.

I also thank Mrs. U. Tipnis for adding to the lively environment in the lab.

I thank the Department of Zoology for support-

ing me during the course of this work by providing a teaching assistantship.

I would also like to thank Shyam for providing everything else that I needed during my stay in Edmonton.

Finally I would like to thank Ravi who has always helped me in being what I am and without whom everything would have been impossible.

TABLE OF CONTENTS

Table of Contents, Cont'd. Page

LIST OF PHOTOGRAPHIC PLATES

LIST OF FIGURES
(Not on the photographic plates)

LIST OF ABBREVIATIONS

SMP = sub-mitochondrial particles

TRU = tripartite repeating unit

P.E.P. = peak enveloping power

F_1-ATPase = coupling factor F_1

OSCP = oligomycin sensitivity conferring protein

EF = exoplasmic fracture face

PF = protoplasmic fracture face

PS = protoplasmic surface

ES = exoplasmic surface

HBHM = heavy beef heart mitochondria

INTRODUCTION

The last decade has witnessed a rapid growth in our understanding of the structure of biomembranes and ideas about lipid-protein interactions and the diversity of protein types in biomembranes have undergone a considerable change. Biological membranes are currently thought to be fluid mosaics (Singer, 1971; Singer and Nicolson, 1972), with globular proteins intercalated into an interrupted lipid bilayer. As with all generalised models of membrane structure, such a picture should be viewed with caution. Especially it should be borne in mind that although the existence of a lipid bilayer may be considered to be well established in some membranes, precise information about the membrane proteins and their mode of interaction with lipids is very scarce (Cherry, 1976). However, irrespective of the particular arrangement of proteins in a membrane, an obvious consequence of fluidity in the bilayer matrix leads to the possibility that the membrane components may be mobile. Lipids may diffuse laterally in the plane of the membrane (Kornberg and McConnell, 1971a; Devaux and McConnell, 1972; Träuble and Sackmann, 1972; Scandella *et al.*, 1972) or by a flip flop process cross from one side of the bilayer to the other (Deamer and Branton, 1967; Kornberg and McConnell,

1971b; Kennedy and Rothfield, 1977). Proteins can also be expected to show both lateral (Frye and Edidin, 1970) and rotational (Wahl *et al.*, 1971; Vanderkooi and Martonosi, 1971) diffusion if they are not held in their place by interactions with each other or with other cellular components, e.g., microtubules and microfilaments.

It is evident from the recent developments in our understanding of the structure of biomembranes that biophysical and biochemical approaches have been rewarding in providing knowledge about their structure. Techniques of nuclear magnetic resonance spectroscopy (Lee *et al.*, 1974; Levine, 1972), electron spin resonance spectroscopy (Likhtenshtein, 1976; Berliner, 1976; Seelig, 1976; Smith and Butler, 1976; Griffith and Jost, 1976; McConnell, 1976), X-ray diffraction (Worthington, 1976; Luzzati, 1976a; Luzzati, 1976b; Luzzati, 1968; Levine, 1973), flourescence spectroscopy (Radda, 1975), neutron beam studies (Worcester, 1976), differential scanning calorimetry and differential thermal analysis (Chapman, 1973; Sturtevant, 1974; Melchoir and Steim, 1976), electron microscopy (Unwin and Henderson, 1975; Zingsheim and Plattner, 1976) and classic techniques of surface science (Sears and Stark, 1973) have provided a wealth of information. Such studies have led to the acceptance of the generalized membrane model described above.

One of the functions of biomembranes is to serve as the reversible transducers of several forms of energy (Mueller, 1969; Chance *et al.*, 1971; Clayton, 1973; Trebst, 1974; Hodgkin, 1963; Haggins, 1972; Inesi, 1972; Rang, 1974;

Kaback, 1974; Skou, 1975; Montal, 1976). One of the major unsolved problems of bioenergetics is to obtain a complete working knowledge of the structure of the membranes of energy transducing organelles. The process of oxidative phosphorylation in which ATP is synthesized by the energy liberated during the substrate oxidation (Slater, 1976; Hatefi *et al.*, 1976; Slater, 1971) takes place in the inner mitochrondrial membrane in eukaryotes. Therefore the study of the structural organization of inner mitochondrial membrane becomes necessary as it would be important in elucidating the mechanism of oxidative phosphorylation.

The inner membrane of mitochondria contains approximately 80% proteins and 20% lipids (Lehninger, 1975). It is composed of many kinds of proteins and phospholipids. Functionally the proteins present in the inner mitochondrial membrane can be divided into three groups:

1. electron transport system, such as flavoproteins and cytochromes (Keilin, 1930; Yakushiji and Okunuki, 1940; Hatefi, 1966);
2. energy transfer system, including mitochondrial ATPase (Pullman *et al.*, 1960) and oligomycin sensitivity conferring proteins (Kagawa and Racker, 1966a; MacLennan and Tzagoloff, 1968); and
3. other proteins, such as carrier proteins of ions and nucleotides.

The inner mitochondrial membrane is functionally and structurally asymmetric and has a specific vectorial organization (Racker, 1970). It is intrinsically permeable to H^+, OH^-, Cl^- and most other simple cations and anions, but has a highly selective permeability for specific metabolites and certain mineral ions because of the presence of specific transport systems (Lehninger, 1975).

Distinct arrays of polyhedral or spherical substructure were observed by Fernández-Morán in 1962, on the surface of "electron transport particles". Later on Fernández-Morán *et al.* (1964) published their detailed studies on these particles and concluded that the cristae of beef heart mitochondria were made up of thousands of particles, each of which had three parts:

1. a spherical or polyhedral head piece (8 to 10 nm in diameter);
2. a cylindrical stalk (about 5 nm long and 3-4 nm in diameter); and
3. a base piece (4 x 11 nm).

These authors thought of base-pieces as forming the integral part of the outer dense layers of the cristae (of the surface that faced away from the matrix). These authors also claimed that negative staining with phosphotungstate was one of the several methods which could be used for the reproducible demonstration of the isolated particle. Isolated particle, when stained with phosphotungstate or shadow-cast, was shown as being a studded ellipsoid appro-

ximately 12 nm in its short dimension and 18 nm in its long dimension (Blair *et al.*, 1963).

Same particles (8.5 nm in diameter) were observed by Stoeckenius (1963) in the negatively stained preparations of mitochondria from *Neurospora crassa*, while a few experiments with the mitochondria from the organs of mammals gave the same results. The stain used was usually phosphotungstic acid (pH 6.8-7.2) and the results obtained with uranyl acetate (pH 7.2) in the presence of ethylenediaminetetraacetic acid (EDTA) were almost identical, although in general less satisfactory. In his electron micrographs, usually, the particles appeared to be separated from the edge of the membrane by a little empty space, although in some preparations at higher magnifications, a narrow stalk, 4.0 to 5.0 nm long, was seen. Chemical fixation by glutaraldehyde destroys at least 95% of the stalked membrane bound particles (Stoeckenius, 1963) (Keyhani, 1972). When the mitochondria were negatively stained after fixation with $KMnO_4$, OsO_4 vapors (Stoeckenius, 1963), or OsO_4 solutions (Keyhani, 1972), the particles were completely absent. In a study conducted by Parsons (1963), projecting subunits were found on the cristae of mitochondria from eight types of mammalian tissue. Malhotra and Eakin (1967) concluded from their study on the mitochondria isolated from the wild type *Neurospora crassa* that the knobs were seen in the negatively stained preparations only when the sucrose isolation medium did not contain EDTA. These

authors suggested that the presence of knobs may have been dependent on the physiological state of mitochondria and procedure of negative staining, and their appearance in the micrographs did not reflect on their capacity for oxidative phosphorylation. Racker and his collaborators soon demonstrated that the inner mitochondrial membrane knobs were ATPase molecules ("coupling factor F_1"; Racker *et al.*, 1965; Racker, 1970; Racker, 1976) and identified the stalk as a factor for conferring sensitivity for a certain antibiotic to the ATPase knobs ("OSCP" = oligomycin sensitivity conferring protein; Racker, 1970; Racker, 1976).

Another coupling factor, F_6 (Fessenden-Raden, 1972) has also been identified, and this in addition to OSCP is needed for the attachment of F_1-ATPase to the membrane (Racker, 1976; Kanner *et al.*, 1976). A hydrophobic protein factor F_0 has been obtained in the form of a membranous preparation from mitochondria (Kagawa *et al.*, 1973). It confers oligomycin sensitivity to F_1 and consists of a proteolipid. It is thought to be responsible for the transmembranous movement of protons (Racker, 1976). OSCP and F_6 are made up of the single polypeptide chains of molecular weights 18,000 and 8,000 respectively (Racker, 1976). Another coupling factor F_2 or factor B (Racker, 1970) has also been described, but it still needs further characterization.

As for the F_1-ATPase knobs, Sjöstrand suggested that these "lollipop"-like structures are artifacts (Sjöstrand, 1968). He proposed that the procedure of negative staining would induce these "lollipop"-like structures because the ATPase molecules would "stick out" due to osmotic shock during specimen drying. However even when the osmotic shock was minimized by negative staining in ammonium molybdate (Muscatello and Horne, 1968; Muscatello and Carafoli, 1969); these "lollipops" were still present. These stalked globules were later on demonstrated in the ultrathin sections of mitochondria and submitochondrial particles, after gluteraldehyde fixation and staining in uranyl acetate (Methanolic) (Talford and Racker, 1973).

The concept that there is a basic repeating unit in the inner mitochondrial membrane came originally from Green and his colleagues (Fernández-Morán, *et al.*, 1964). These repeating units were described as tripartite structures, each consisting of a polyhedral or spherical headpiece (8.0 to 10.0 nm in diameter), a cylindrical stalk (about 5.0 nm long and 3-4 nm wide), and a base-piece (4 x 11 nm). However, later on Green proposed the electromechanochemical model (EMC model) for the energy transduction in mitochondria, and again invoked the existence of an inner membrane repeat unit, in which the component proteins assume metastable conformations (Green, 1972; Green, 1974). Green also proposed a mitochondrial super-

molecule (for his EMC model) which consists of five complexes (Green, 1974): the four complexes of the electron transfer chain and a central unit, the tripartite repeating unit (TRU), which contains systems involved in both ATP synthesis (the F_1-ATPase) and active transport. The complexes including the headpiece of TRU, all span the membrane from matrix to the intracristal side (Green, 1974).

In the present work Green's hypothesis has been tested by investigating the sub-unit structure within the plane of the inner mitochondrial membrane (isolated in the form of the vesicular SMP), obtained from beef heart mitochondria. The theoretical basis underlying the experiments that were carried out to achieve the above-mentioned objective, is described below.

A membrane is a three-dimensional structure and a schematic drawing of the single membrane is given in Figure 1. The electron density distribution of this membrane can be represented by t(r), where r represents real space coordinates (Worthington, 1976). This t(r) can be written as

$$t(r) = t(x)t(y,z),$$

(Worthington, 1976), where t(x) and t(y,z) are lameller and sub-unit structure respectively. The one-dimensional electron density distribution in a direction at right

angles to the membrane surface is referred to as the lameller structure. The sub-unit structure refers to the structure within the plane of the membrane (Worthington, 1976).

In an X-ray diffraction experiment, diffractions arising from t(x) and t(y,z) can be distinguished as the X-ray beam parallel to the surface of the membrane gives rise to lameller diffraction, whereas when the X-ray beam is perpendicular to the surface of the membrane, it will give rise to sub-unit diffraction.

In the case of the inner mitochondrial membrane, if there is any regularly repeating structure within the plane of the membrane as has been proposed by the workers cited above, this regular surface lattice must be represented in the optical Fourier transform of the image of SMP in electron micrographs. This situation is analogous to the X-ray diffraction experiment, designed to obtain the sub-unit diffraction from the membrane. In the optical diffraction, a laser is used instead of X-rays and the membrane specimen is replaced by its electron micrograph. In the present study, the technique of optical diffraction was employed to reveal all the periodicities present in the electron micrographs, as it provides the optical Fourier transforms of the micrographs. Klug and Berger (1964) first suggested the application of optical diffraction for the analysis of periodic structures in electron micrographs. Later on Klug and his coworkers (Klug and

DeRosier, 1968; DeRosier and Klug, 1968) developed two novel methods which enable an electron microscopist to extract phase information in the micrographs. (Optical diffraction pattern records only the intensity $|\psi|^2$ of the Fourier components of the specimen and not the phases). The information that can be obtained from the optical diffraction pattern (optical Fourier transform) of an object is quite extensive. Unit-cell dimensions can be measured much more accurately from an optical diffractogram than from the direct measurements on the micrograph (Berger, 1969; Sternlieb and Berger, 1969). By employing optical diffraction one can get separate details of periodic character from the substrate noise (phase contrast induced granulation). Symmetry elements are revealed in the optical diffraction pattern of the micrograph (Klug and Berger, 1964).

The electron micrographs of the freeze-etch replicas were also processed for optical diffraction, to investigate the arrangement of the "intramembranous particles" on the fracture faces of SMP. Purpose of this exercise was to find information regarding the order of arrangement of these particles in the hydrophobic interior of the inner mitochondrial membrane (SMP).

MATERIAL AND METHODS

Beef heart was chosen as the source for obtaining the mitochondria because (1) it is available in bulk quantities and is cheaper, and (2) beef heart mitochondria are more stable over long storage periods. All the chemicals other than potassium succinate and PTA (which were purchased from Fisher Scientific Co.) were obtained from Sigma Chemical Co.

Isolation of Mitochondria

The mitochondria were isolated from the beef heart by the method given by Smith (1967). Two beef hearts were obtained from a slaughter house within one to two hours after the animals were sacrificed. To ensure the cooling of the tissue for transport to the laboratory, the hearts were placed in ice. All subsequent operations were carried out at 2-4°C. The fat and the connective tissue were trimmed from the heart and then the tissue was chopped into small pieces. Approximately 300 grams of the chopped tissue was passed through the meat grinder which was maintained at 4°C. The meat grinder had plate holes approximately 4-5mm. in diameter. Thus obtained mince was placed in 400 ml. of 0.25M sucrose and 0.01M Tris-HCl, pH 7.8. The pH of the suspension was adjusted to 7.5 as rapidly as possible with 2M Tris (pH 10.8, unneutralized). This neutralized ground heart mince was placed in a double

layer of cheesecloth and was squeezed free of the sucrose solution. About two hundred grams of this ground, neutralized heart tissue were suspended in 400 ml. of 0.25M sucrose, 0.01M Tris-HCl, pH 7.8; 1 mM Tris-succinate, and 0.2 mM EDTA (this solution will be referred to as the sucrose solution). In a glass homogenizing vessel, fifty milliliters of the suspension was placed, and a loose-fitting pestle driven by the heavy-duty drill at 1400 rpm was inserted into the vessel for one pass of 10 seconds and two passes of about 5 seconds each. The rest of the suspension was homogenized in a similar way, and the final homogenate was adjusted to pH 7.8 with the addition of 1 M KOH. The homogenate was centrifuged for 20 minutes at 1200 g (Sorvall centrifuge RC2-B, rotor SS34 at a setting of 3250 rpm) in order to separate unruptured muscle tissue and nuclei. The supernatant solution was slowly decanted, taking care not to disturb the loosely-packed fluffy layer. To remove lipid granules, it was filtered through two layers of cheesecloth, and the pH of the suspension was again brought to 7.8 with 1M KOH. This suspension was centrifuged for 15 minutes in a type 40 rotor of the Beckman L3-40 centrifuge at 26,000 g (22,000 rpm). A pellet resulted, which consisted of three distinct layers: (1) a light, loosely-packed buff-colored layer (light beef heart mitochondria), (2) a dark brown layer (heavy beef heart mitochondria), and (3) a tiny brown-black button at the bottom of the tube. The top layer, which consists of dam-

aged mitochondria was discarded by decanting about 20-25 ml. of the supernatant solution and then gently shaking the sucrose solution in the centrifuge tube. Thus the loosely packed damaged mitochondria were dislodged and the mixture was decanted out. Some light beef heart mitochondria adhered to the sides of the tube, which were removed with the aid of a glass stirring rod. The dark brown layer of the heavy beef heart mitochondria was then dislodged by a glass stirring rod, mixed with 10 ml. of sucrose solution, and decanted, leaving behind the brown-black pellet. This mitochondrial suspension was homogenized in a tight fitting teflon homogenizer, with two passes, each of 5 seconds at 1400 rpm.

The volume of the homogenate was made up to 180 ml. with sucrose solution, pH was readjusted to 7.8, and the suspension was again centrifuged at 26,000 g for 15 minutes. The resulting pellet had three layers; a small top, a large middle, and small bottom layer. Only the middle dark brown layer was collected as described above. The mitochondrial suspension was homogenized, and the volume was adjusted to 60 ml with the sucrose solution. The pH was adjusted to 7.8. This suspension was centrifuged at 26,000 g for 15 minutes. This time again the dark brown middle layer was collected, suspended in a small volume of sucrose solution, and homogenized. The protein concentration was adjusted to 20-40 mg protein per milliliter. Protein determinations were done by Lowry's method (1951)

and the average yield of heavy beef heart mitochondria (HBHM) was about 1 mg protein per gram of initial mince.

Preparation of Sub-mitochondrial Particles (SMP)

The sub-mitochondrial particles from beef heart mitochondria were obtained by the method of Hansen and Smith (1964). HBHM were isolated as described above, and were suspended in a solution 0.25M in sucrose, 0.01M in Tris-HCl, pH 7.8, 1mM in ATP, 1mM in $MgCl_2$, and 1mM in potassium succinate (this solution is abbreviated as STAMS), at a protein concentration of 30 mg/ml; pH of the suspension was adjusted to 7.8 with 1N KOH. This suspension was centrifuged at 26,000g for 15 minutes. The dark brown middle layer of HBHM was collected as described before, and suspended at a protein concentration of 30 mg/ml in a solution 0.25M in sucrose, 0.01M in Tris-HCl (pH 7.5), 1mM in ATP, 1mM in potassium succinate, 5mM in $MgCl_2$, and 10mM in $MnCl_2$. The pH of the solution was adjusted to 7.5 with either 1N HCl or KOH. Aliquots of about 15 ml. were placed in a tube, kept in ice, and subjected to 10Kc sonic irradiation for 2 minutes from a sonifer (Braunsonic 1510) at a power output between 100 to 150 Watts (P.E.P.). The pH was adjusted to 7.5 and the resulting suspension was centrifuged at 14×10^4g-min. (20,000 rpm, 7 minutes, No. 40 rotor in a Beckman L3-40 ultracentrifuge). The supernatant was collected by decantation

and was centrifuged at 40,000 rpm in a Beckman Type 40 rotor for 45 minutes in a Beckman L3-40 ultracentrifuge (105,000 × g). As a result of this a tightly packed reddish brown pellet was obtained. The surface of the pellet was rinsed with a few milliliters of a solution 0.25M in sucrose and 0.01M in Tris-Hcl, pH 7.5, and the pellet was suspended to a protein concentration of about 20 mg/ml in sucrose-Tris solution described above. Protein determinations were done by the method of Lowry (1951).

Negative Staining

For negative staining a drop of the SMP suspension diluted to approximately 1 mg protein/ml, was placed on the formvar and carbon-coated grids and stained with 2% phosphotungstic acid (PTA), pH 7.1. Phosphotungstic acid was used because it is thought to be an effective stain, for the many polar atoms in its periphery impose an ordered structure on adjacent water molecules and leave the structure beyond it undistorted so that water can evaporate with little damage to the surface of the molecule (Blundell and Johnson, 1976).

Freeze-etching of SMP

a. Freeze-etching of glycerolated SMP

For freeze-etching in glycerol, the SMP suspension was centrifuged for 45 min. at 40,000 rpm in a Type 40

rotor in a Beckman L3-40 ultracentrifuge. The resulting pellet was suspended in 20% glycerol at the protein concentrations of 10-15 mg/ml. After 2 hours in glycerol solution, drops of sample were frozen in liquid Freon 22 and transferred to a Balzers freeze-fracture device and fractured at -100°C as described by Malhotra and Tewari (1973). The preparations were etched for 70 seconds with a liquid N_2 cooled knife right over the specimens at a vacuum of 1×10^{-6} torr and replicated with platinum-carbon. The replicas were soaked in chromic acid overnight, washed for 1 hour in household detergent solution, followed by three washings in distilled water and eventually these were picked up on the formvar-coated copper grids.

b. Freeze-etching in water

The SMP suspension was centrifuged for 45 minutes at 40,000 rpm in a Type 40 rotor in a Beckman L3-40 ultracentrifuge. The resulting pellet was suspended in distilled water at a concentration of approximately 5 mg protein/ml and centrifuged again at 40,000 rpm for 45 minutes, in a Type 40 rotor in a Beckman L3-40 ultracentrifuge. The pellet so obtained was suspended in distilled water at a protein concentration of 10-15 mg/ml. Drops of the sample were frozen in liquid Freon 22 and processed for freeze-etching as described before in the case of the SMP suspended in 20% glycerol.

Electron Microscopy of Negatively Stained SMP Preparations

In the high resolution electron microscopy of biological or organic specimens, the radiation damage poses a very severe limitation over the obtainable resolution. In spite of the continual developments in the instrumental resolving power and the applications that have been made with these improvements to the inorganic materials, the best resolution of periodic structure obtained with stained biological specimens is usually 2 to 3 nm. The resolution, attained with the unstained biological specimens is far worse than the above-mentioned value. However, a few exceptions to the general limitations on resolution in organic materials have been found, but these exceptions always occur in materials that are unusually resistant to the radiation damage (Glaeser, 1975). From a simple calculation it can be shown that the usual exposures needed in high resolution electron microscopy lead to a radiation dose of 10^{10} to 10^{11} rads being deposited in the sample (Glaeser, 1971; Glaeser *et al.*, 1971; Grubb and Keller, 1972). On the other hand, a dose of 10^{9} rads is sufficient to destroy the original properties of most organic materials and a dose of 10^{6} rads will inactivate most of the enzymes and kill the most resistant of all living things (Glaeser, 1975). An idea of the severity of radiation damage can also be obtained from the following example (Stenn and Bahr, 1970): In a 0.1μ thick

organic specimen, at 100kV a single electron sustains approximately one inelastic collision in passing through it. Each collision has an energy yield of the order of 32eV (the energy yield of a C-C single bond is of the order of 5eV). At a magnification of 10,000x, a current density of at least 10^{-2} amp/cm^2 is required and from this it has been calculated (Stenn and Bahr, 1970) that energy absorbed by 1g of specimen in a 1s exposure is sufficient to bring 20g of ice to steam.

An estimate of the electron fluxes to "see" the molecular detail has been made by Glaeser (1971). The detectability of an object feature of the characteristic dimension d is determined by the ratio of signal to noise in the measurement. In order to record the image features with low contrast under the conditions of severely restricted exposure, the signal-dependent noise, associated with statistical fluctuations in the intensity from one area to another in the image, must be given careful consideration (Glaeser, 1971; Glaeser, 1975). Image contrast can be defined as the ratio between spatial variations in the intensity and local average of intensity (Glaeser, 1975):

$$C = \frac{\Delta I}{\langle I \rangle} \qquad \ldots (1)$$

In the above equation C denotes inherent image contrast. The incidence of the electrons at the image plane is a

random process (Glaeser, 1971). If the total number of electrons passing into a given image "point" (picture element) is n, then the statistical fluctuation, or "counting error" is $\sqrt{n}$ (Glaeser, 1971). It is beneficial to express this fluctuation in terms of the following parameters:

(1) the area of picture element, d^2;

(2) the current density through the object, j;

(3) the "integration time" or exposure time, t; and

(4) the fraction of electrons passing through the specimen that actually enter the lens aperture and contribute to the image, f (Glaeser, 1971). And thus,

$$n = fjtd^2 \qquad \ldots (2)$$

In case of limited exposure, a certain statistical fluctuation occurs in the particle flux from one image point to another, leading to the generation of spurious structure, or spatial noise, with contrast (Glaeser, 1971):

$$C' = \frac{\Delta n}{n} \qquad \ldots (3)$$

where

$$\frac{\Delta n}{n} = \frac{1}{\sqrt{fjd^2t}} \qquad \ldots (4)$$

Therefore, in order to "resolve" a low contrast image feature, the inherent contrast must exceed the statistical fluctuations by the minimum acceptable signal to noise-ratio, S/N. It leads to the following inequality (Glaeser, 1971):

$$Cd \geq \frac{S/N}{\sqrt{fjt}} \qquad \ldots (5)$$

According to this equation the product of resolution and contrast must exceed a certain constant, which in turn is determined by the conditions of measurement (f, j, and t) and by the conditions of analysis (minimum acceptable S/N) (Glaeser, 1971). Therefore, to record some object feature with contrast C at the resolution d, the integrated flux density jt must be greater than or equal to $(S/N)^2/C^2d^2$. For a specimen with a value of S/N = 5, the value usually quoted for the visual perception of structure (Rose, 1948), and an inherent image contrast C = 0.1, the minimum resolution attainable with a flux density of 10^{17} electrons/cm^2 (the maximum permissible dose for negatively stained catalase crystals) is of the order of 1.6nm (Glaeser, 1971). To resolve up to 0.5nm, a current density of 10^{18} electrons/cm^2 is needed which would totally destroy the specimen. Thus the radiation damage leads to a paradoxical situation. In order to achieve high resolutions, we need greater electron fluxes, but these electron fluxes would destroy the organic specimen's structure.

Disordering effect of the high vacuum in the electron microscope also causes extensive damages to the biological or organic specimens (Stenn and Bahr, 1970).

The suggestion has often been made that the problem of radiation damage would be greatly reduced if the specimens could be examined in a vacuum of 10^{-8} torr or better. This suggestion is based on the observation that the specimens undergo dramatic modifications and it is associated with residual gases in the microscopes at a pressure of 10^{-5} to 10^{-6} torr. Specimen contamination and specimen etching are also one of the common problems encountered in preserving the specimen structure in the electron microscope.

Negative staining alleviates these damaging effects to some extent. Salts used in the negative staining lose water quicker than the protein molecules in the drying process and hence preserve the structure of the hydrated protein (Horne and Whittaker, 1962; Johnson and Horne, 1970), and form a glass around the specimen which is likely to prove more resistant to the beam damage than the biological molecule alone. It was due to this reason that in the present study, the negative staining method was employed to visualize the SMP preparations in the electron microscope. The electron microscope was also suitably modified to provide low-dosage conditions for the electron-microscopy of the negatively stained SMP preparations. The overall objective was to reduce the specimen damage, due to the electron beam, in the electron microscope.

The following method was used for taking the bright field electron micrographs of the negatively stained

SMP preparations. A Philips EM 300 electron microscope, equipped with a liquid N_2 cooled anti-contamination device, operating at 100kV with 50μm (first) and 50μm (second) condenser apertures was used. No objective aperture was used. A narrow coherent illuminating beam could be obtained by exciting the first condenser lens, strongly. At first the grid was scanned at low magnifications using very low illumination levels, just enough to reveal the outline of the structures. Once a suitable area was found, it was brought on the optical axis of the electron-microscopy (the marked spot on the large viewing screen) and the magnification was increased to the desired level. The specimen was then moved slightly using the translation controls, so that the area of interest was removed far from the center of the screen. Following this a narrow coherent illuminating beam was obtained, as described above, to enable the focusing to be done. The beam was then expanded to give the desired intensity on the screen (this intensity of illumination was kept as low as possible with the photographic exposure times kept at 4-16 sec.) and the area of interest was brought back and placed on the optical axis of the electron microscope and photographed.

Electron Microscopy of Freeze-etch Replicas

Freeze-etch replicas were examined routinely in a Philips EM300 electron microscope operating at 80kV with a liquid N_2 cooled anticontamination device using

300μm (first) and 300μm (second) condenser apertures and a 25μm objective aperture.

Optical Diffraction

Optical diffraction experiments were carried out on a Polaron electron micrograph optical-diffractometer model M802. Optical elements in this optical diffractometer are mounted on a 3 metre length of double rail precision optical bench. The optical diffractometer lens system shown in Figure 2 can be easily divided into three parts:

a. the electron micrograph illuminating system;
b. the transform imaging system; and
c. the image reconstitution system.

a. Micrograph illuminating system

A 2 milliwatt helium-neon laser provides a source of coherent light of λ = 632.8nm. It gives a beam of about 2mm cross-sectional diameter, and it is mounted on adjustable legs. A spatial filter, SP, consisting of microscope objective fitted with the front face of laser and adjusable iris diaphragm is employed to prevent any extraneous light from laser. The rays become divergent in passing through the objective and are converted by a planoconvex lens B to a collimated beam of light approximately 1 cm. in diameter incident on the electron-micrograph C. The electron micrograph is suitably masked to expose the par-

ticular area of interest only, and mounted on a mechanical stage which provides adjustments for selecting any area on the micrograph.

b. Transform imaging system

A plano convex lens D is used to image the optical Fourier transform of the micrograph. A two-lens telephotosystem consisting of lenses E and F is employed to magnify the image of the transform. The transform can be viewed by placing a ground glass screen in the mask holder G and recorded with 5 x 4 Polaroid Land camera back provided. The polaroid print of the transform is used for making a metal mask which allows the primary beam and selected diffracted beams to go into the image reconstruction system. The mask is fitted in holder G in image reconstitution experiments.

c. Image reconstitution system

The rays which pass through the mask are reconstructed using lens H and J. Together these lenses form a telephoto system which is reversed and symmetrical with respect to lenses E and F. Lens K, which is final, is a power projecter lens. Again, the reconstituted image may be viewed using the ground glass screen or can be recorded by the camera.

However, in the present study, where the transform (optical Fourier transform) was of main interest, the lenses H, J and K (image reconstitution lenses) were re-

moved and other lenses were rearranged on the entire optical bench to increase its magnification.

Both the negatives of the electron micrographs of negatively stained SMP (at the magnification of x 25,000 --40,000) and their enlarged transparencies (at the magnification of x 60,000--80,000) were used in the optical diffraction experiments. These were suitably masked to expose only the particular areas of interest and were used as objects in the optical diffractometer. A total of 20 different specimens were analyzed.

Micrographs of the freeze-etch replicas of SMP preparations were enlarged to a final magnification of x 242,000. Holes were punched in the micrograph at the locations where there seemed to be particles on the convex fracture face of SMP. Then the micrograph was kept on a black paper with its face down, so that the holes appeared black on white background. This was then photographed on a Kodak Panatomic X film. The resulting negative reduced the size of the mask (representing the arrangement of particles on the convex fracture face of a SMP) 19 times and was finally used as an object in the optical diffractometer. A total of 10 specimens were analyzed. Photographic negatives of the optical diffraction patterns (optical Fourier transforms) were used for measurements.

RESULTS

Negative Staining

a. Relationship between the electron microscope image and the specimen

In the process of negative staining the specimen is surrounded by an aqueous solution of an electron dense salt (the negative stain) which dries out into a thin film. This thin film, in effect, is an amorphous electron dense 'glass' (Horne and Whittaker, 1962) in which the specimen is buried. The negative stain penetrates into the hydrophobic regions of the biological specimen and the resulting image in the electron microscope reveals the unpenetrated regions as relatively electron-transparent structures against an electron dense background. Thus the amplitude contrast is provided by the scattering of electrons by the stain (Blundell and Johnson, 1976).

In the electron microscopy contrast is achieved by both the amplitude contrast and by the phase contrast effects which are created by contributions from defocusing and spherical aberration of the objective lens. Phase contrast plays the predominant role at medium and high resolutions. Since the Fourier transform of the image displays these phase contrast effects more simply than the image itself (Erickson and Klug, 1971), these can be

readily investigated with the help of an optical diffractometer or computer transforms. According to the wave theory of image formation, the effects of defocusing and spherical aberration are attributed to a phase shift ($\chi\{\alpha\}$) which occurs at the diffraction plane of the microscope, in the scattered electron wave. It is a function of scattering angle α and is given by

$$\chi(\alpha) = 2\Pi/\lambda(-\tfrac{1}{4}C_s\alpha^4 + \tfrac{1}{2}\Delta f\alpha^2) \quad \ldots (6)$$

where C_s is the coefficient of spherical aberration and Δf is the defocusing (positive for a weak or underfocused lens) (Erickson and Klug, 1971). Transform of the phase contrast image, T^i_{ph}, is related to the transform of the object, $T^0(\alpha,\phi)$ by the expression:

$$T^i_{ph}(\alpha,\phi) = -T^0(\alpha,\phi)A(\alpha)f(\alpha)\mathrm{Sin}\chi(\alpha) \quad \ldots (7)$$

where $A(\alpha)$ accounts for the effect of an objective aperture and is called aperture function ($A[\alpha] = 1$ if $\alpha \leq$ defining aperture angle; $A(\alpha) = 0$ elsewhere), α is the scattering angle, $f(\alpha)$ is the atomic scattering factor for the elastic scattering of electrons, and ϕ is the azimuthal coordinate (Erickson and Klug, 1971). This equation tells us that the relation of the object to the image formed in the presence of aberrations is very simple and direct if expressed in terms of Fourier transforms. According to

this expression the image transform is directly proportional to the true object transform, modulated by three factors. Most important factor among the three factors is $\sin\chi(\alpha)$, which is also called as the transfer function (Hanzen, 1971).

The transfer function will have the following effects on the terms corresponding to a spatial resolution of λ/α: (a) if $\sin\chi(\alpha)$ is close to 1, then these terms would provide their full weight to the Fourier transform and details corresponding to this resolution would be faithfully imaged; (b) if $\sin\chi(\alpha)$ is close to zero, then the terms of spatial resolution will be removed from the transform and will not contribute to the final image; (c) if $\sin\chi(\alpha)$ changes sign then terms corresponding to this resolution will contribute to the final image with reverse contrast leading to the risk of false image. Therefore it is required that $\sin\chi(\alpha)$ be relatively invariant over the range of resolutions of interest to us. Curves for $\sin\chi(\alpha)$ for different degrees of underfocus were computed by Erickson and Klug (1971). It was concluded that 90nm underfocus would be a favourable choice for imaging details between 2 to 0.5nm resolution, while a greater degree of underfocus would be suitable for imaging details between 5 to 2nm range. Erickson and Klug (1971) also examined the effect of transfer function in real images (negatively stained catalase crystals) and concluded that at $\Delta f = 540$nm many of the high resolution components are enhanced and

micrograph contains more detail and contrast. At this underfocus value, the phase contrast effect is sufficient to increase the transfer function for periodicities in the range of 2 to 5nm by about five times to that of the in-focus image. Since this range of detail is of particular interest in protein studies, 500nm was thought to be the optimum underfocus setting for such work. This is a very important study because it provides insight into one of the most important aspects of image formation. In the present work too, most of the electron micrographs are moderately underfocused. In the present work, the electron micrographs of negatively stained SMP were taken at two underfocus settings: (a) at ~100nm underfocus (for imaging details between 2.0 to 0.5 nm resolution); (b) at ~550nm underfocus (for enhancing the high resolution components in the range 2.0 to 5.0 nm. It was in accordance with the conclusion drawn by Erickson and Klug (1971) with respect to the implication of their work in biological electron microscopy. In their own words,

> Finally it is comforting to be able to confirm quantitatively that the moderately underfocused micrographs used in most biological electron microscopy are valid images, frequently the best possible in terms of resolution and contrast, with no artifacts in the low and medium resolution range of interest.

b. Negatively stained SMP and cristal membrane fragments

In a typical SMP preparation, negatively stained, such as one shown in Figure 3, knobs approximately 10nm in

diameter can be easily identified on the inner mitochondrial membrane vesicles (SMP). These inner mitochondrial membrane vesicles have the inner-mitochondrial membrane in the inside-out configuration, and these vesicles (SMP), therefore enable F_1-ATPase knobs to be visualized. These knobs look more like polyhedral structures. It was Racker ('70, '76) who first of all demonstrated that the knobs present on the SMP are F_1-ATPase ("coupling factor"). In most cases these knobs appear to be attached to the membrane by the stalks (Figure 4). These stalks are approximately 6nm long and 3nm wide, and correspond to the oligomycin sensitivity conferring proteins ("OSCP", Racker, 1970). On the edge of the SMP, the F_1-ATPase knobs can be very clearly seen to be attached by the stalks to the SMP, in most of the cases. These stalks are separated from one another by approximately an ~11nm-wide gap, as measured on the edges of the negatively stained SMP.

Frozen beef heart mitochondria, when they are subjected to swelling and alternate freezing and thawing in 10mM Tris chloride (pH 8.0), their cristal membranes undergo "tubularization" (Green, 1976). Results from such a phenomenon are shown in Figure 5. Regular-looking arrays of knobs connected to the membrane by the stalks, on either side of the "tubular" membrane, are discernable. This tubularization may be due to the transition of a single flat continuous membrane sheet to a large number of interconnecting tubules (Green, 1976). According to this

author tubularization of the inner mitochondrial membranes means that the components of this membrane can exist in either of two states--the "two-dimensional" state of the flat membrane sheet and the "three-dimensional" state of tubular evaginations. In such structures, described as "tubular" by Green, the knobs have the diameter of 11.0nm (corresponding to the F_1-ATPase knobs) and the stalks are ~6nm long and ~3nm wide. The distance between the two stalks on the "tubular" membrane is ~11nm.

Freeze-etching

a. Interpretation of freeze-etch replicas

The evidence was first presented by Branton and his coworkers in support of their hypothesis that during "freeze-etching", the fracture plane passes through the interior of the biological membranes, so that the inner faces become exposed (Branton, 1966). Face views of the fractured membranes show particles of ~10nm diameter. Their number is subject to variation from one membrane type to the other. Branton argued that these particles belonged to the membrane interior. It was observed that upon etching, fractured membranes frequently display a narrow ridge ~3nm thick. Where the face view changes into cross-fracture, the ridge is seen to be continuous with one of the two parallel ridges that form the usual appearance of cross-fractured membranes. Therefore it was concluded

that the membrane was split. Similar argument has also been applied to the swollen nerve myelin, rod outer segment membranes, and swollen lecithin lameller phases (Branton, 1967, Clark and Branton, 1968; Staehlin, 1968). After considering actual dimensions and spacings of the ridges, it becomes clear that an ~5.5nm-wide gap must exist between them. Langmuir-Blodgett technique (Langmuir, 1917; Blodgett, 1935; Langmuir, 1939) has been employed to assemble radioactively labelled bilayers and multilayers. These were frozen and split and the radioactivity of the separated layers was measured. The results thus obtained are explainable only by assuming that assemblies split along a plane defined by the methyl end groups of the individual monolayers (Deamer and Branton, 1967). After fracturing and shadowing under the conditions of freeze-etching (-100°C), very smooth surfaces were noticed. Only a few particles could be found on these surfaces. Similarly membranes which have little or no protein, generally display smooth fracture faces as in the nerve myelin (Branton, 1967; Malhotra *et al.*, 1975), liposomes (James and Branton, 1971) and lameller lipid phases (Deamer *et al.*, 1970). However, more information about the nature of the surface revealed after freeze-fracturing was obtained by experiments employing chemical prefixation. Aldehyde fixation which cross-links the proteins, did not bring about any change in the appearance of the membranes after freeze-fracturing and etching. However, an improvement in their

overall mechanical stability was noted (Jost, 1965; Branton and Park, 1967; Tillack and Marchesi, 1970). When the aldehyde-fixed membranes were subjected to lipid extraction prior to the freeze-fracturing and etching, the splitting of membranes was abolished completely. Although the trilameller structure could still be seen in the thin sections (Park and Branton, 1966; Fleisher *et al.*, 1967; Branton and Park, 1967). These results clearly indicate that the lipids or lipid regions are required to achieve freeze-fracturing of the membranes along an inner plane.

Deamer and Branton (1967) have proposed an hypothesis to explain the splitting behaviour of the biomembranes. They explain their arguments on Kauzman's (1959) thermodynamic considerations of the temperature dependence of the energy of hydrophobic bonding. Freezing is known to weaken the hydrophobic bonds and so the hydrophobic interior of the biomembranes becomes more susceptible to splitting in the frozen state than any other zone. However since the frozen membrane is not in a thermodynamically equilibrium state, their argument should be weighed with caution.

Experiments with the membrane surface markers (covalently bound Ferritin or attached F-Actin) demonstrate that these markers can only be seen after etching; they never appear on cleaved membrane faces (Pinto de Silva and Branton, 1970; Tillack and Marchesi, 1970). This lends strong support to the membrane splitting hypothesis. By

employing the techniques for the production of complimentary replicas from both (complimentary) fracture faces of a membrane (Sleytr, 1970; Wehrli *et al.*, 1970; Chalfont and Bullivant, 1970), it was found that both fracture faces were unetchable. It can be simply explained on the basis of the membrane splitting hypothesis.

Branton (1967; 1971) has argued that the molecular correlates of the membrane intercalated particles occurring within freeze-fractured biomembranes, are proteins. It has been shown that they are pronase sensitive and their occurrence is influenced by the "metabolic activity" of a cell or membrane type.

Wallach and Zahler (1966) were the first to point out the possibility and likelihood of hydrophobic protein-lipid interaction in biomembranes. A large amount of evidence has accumulated in the last few years regarding the membrane intercalated particles and now the idea is widely adopted that these membrane intercalated particles represent proteins (including the polypeptides and oligomers (Bullivant, 1974; Bretscher and Raff, 1975). Recently (Branton *et al.*, 1975) a nomenclature for the freeze-etching has been proposed which is simple and uniform to describe the various fracture faces and surfaces. According to this scheme of nomenclature, for any membrane that can be split, the half closest to cytoplasm, nucleoplasm, chloroplast stroma or mitochondrial matrix is designated as "protoplasmic half" abbreviated as P; the half closest

to the extracellular space, exoplasmic space, or endoplasmic space is designated as extracellular, exoplasmic or endoplasmic half, abbreviated as E. E is also used to designate the half membranes closest to the space between the inner and outer membranes of mitochondria.

After labelling the half membrane as P or E, the particular aspect seen in the electron microscope can be recognized as a true surface of the membrane or as a fracture face. The surface is named either PS or ES and it is the hydrophilic portion of the membrane usually revealed after etching; the fracture face is designated as PF or EF.

b. Freeze-etching of SMP

Sub-mitochondrial particles are inside-out inner mitochondrial membrane vesicles, obtained from the mitochondria. Therefore, in SMP, the face of the inner mitochondrial membrane, which is closest to the mitochondrial matrix in intact mitochondria, faces the outside of the vesicle. And the outer surface of the inner mitochondrial membrane in intact mitochondria faces the inside of the vesicle in SMP.

In a sub-mitochondrial particle, therefore, the protoplasmic half of the inner mitochondrial membrane faces towards the exterior of the vesicle while the exoplasmic half faces towards the interior of the vesicle (Fig. 6a). For the sake of explanation the sub-mitochondrial particles

can be considered to be the vesicles of varying size. During the fracturing, the fracture plane "hits" those vesicles which are within the reach of this plane. The membrane of these vesicles splits in half between the phospholipid leaflets thus revealing, on a profile in the form of a spherical surface, an internal fracture face of the membrane studded with particles. If the plane hits the vesicle above the equator, a convex fracture surface is formed; if it hits below the equator, the surface is concave (Weibel, Losa and Bolender, 1976). In SMP, the convex fracture face is the exoplasmic fracture face (abbreviated as EF) and the concave fracture face is the protoplasmic fracture face (abbreviated as PF). The corresponding etched true surfaces are called exoplasmic surface (the ES) and protoplasmic surface (the PS) (see Figure 6b).

i. Freeze-etching of glycerolated SMP

The total number of replicas examined was 40 and they were selected from 18 freeze-fracture experiments.

Typical fracture faces revealed after freeze-fracturing and etching of SMP in 20% glycerol are exhibited in Figures 7, 8 and 9. Both convex and concave fracture faces were obtained. No true surface was exposed as a result of the etching of glycerolated SMP preparations. The membrane intercalated particles are present on both the convex and the concave fracture faces. The convex fracture face is the exoplasmic fracture face (EF) and the

concave fracture face is the protoplasmic fracture face (PF). The intramembranous particles with diameters ranging from about 5.0nm to 16.0nm are present on both the fracture faces. It seems that the convex fracture face (EF) has a lower packing density of particles as compared with the packing density of particles on the concave fracture face (PF). There are approximately 1300 ± 300 particles/μm^2 in the convex fracture face and about 2000 ± 200 particles/μm^2 in the concave fracture face. It indicates the asymmetry in the particle distribution in the two halves of the membrane.

The size distribution of the particles is given in Figure 11. Most of the particles fall in the size range 10-12nm, but there is a significant number of particles in the 7 to 10nm range too. The significance of this distribution of intramembranous particles in respect of the known composition of the inner motichondrial membrane is discussed on p. 51. On the concave fracture face, a few of the particles are sometimes seen to be arranged in some kind of irregular rows, and their pattern is uneven (Figure 10).

ii. Freeze-etching of SMP in water

When the sub-mitochondrial particles are suspended in water and subjected to freeze-fracturing and etching, at least two types of membrane faces must be exposed in principle. One is the fracture face containing the

membrane-intercalated particles of the hydrophobic interior and the other is the etch face (surface). A typical convex fracture face (EF) exposed in the freeze-fracturing and etching of SMP suspended in distilled water is shown in Figure 12. It displays typical intramembranous particles ranging from about 5.0nm to 16.0nm in diameter. The packing density of these particles is about 1600 particles/μm in this fracture face.

However, of the total of 38 replicas (obtained from 15 freeze-etching experiments) examined, only one replica showed two SMP with etch surfaces. The main reason for getting the etch surfaces with such difficulty seems to lie in the very small surface area of the submitochondrial particles in the suspension. On fracturing, most of the surface area of the SMP is fractured, and it appears that very little area is left for the subsequent etching. And this, perhaps, renders the probability of obtaining meaningful etching very low.

The etch surface (PS) is smooth and does not show the presence of any particles on it (Figure 12). On the contrary, a negatively stained preparation of the same SMP preparation displays the typical ~10nm F_1-ATPase particles (knobs) attached to the membrane. This observation raises some very interesting questions. Why does the F_1-ATPase not show up as the particles on the etch surface (PS) of the inner mitochondrial membrane in the freeze-etch replica of the SMP preparation? Is it being lost in

the freeze-etching experiment, from the surface of SMP? Could it be possible that the negative staining is causing the "lollipop"-like appearances of F_1-ATPase on the SMP? These questions are discussed on p. 42.

Optical Diffraction Studies

a. Negatively stained SMP preparations.

A typical optical Fourier transform of the electron micrograph of a negatively-stained sub-mitochondrial particle is displayed in Figure 13b. The corresponding electron micrograph of the negatively stained sub-mitochondrial particle is shown in Figure 13a. Only a part of the surface (the image) of the sub-mitochondrial particle was subjected to optical diffraction. The remainder of the area was covered. This was achieved by using a black mask with a circular hole in it, which allowed the desired area to remain exposed to the laser beam, in the optical diffraction experiment. This area is shown under the circle in Figure 13a. Therefore, the optical Fourier transform of the electron micrograph (Figure 13b) also contains the Fraunhofer diffraction pattern of a circular hole; which displays a central peak called the airy disk, surrounded by successively weaker rings. In some cases instead of using a circular mask, a rectangular mask was used. For example, a rectangular mask was applied to the electron micrograph of a negatively stained SMP (Figure 14a) to leave open a rectangular area and mask out the

remainder of the area. The corresponding optical Fourier transform is shown in Figure 14b. The transform contains the Fraunhofer diffraction pattern of a rectangular opening too, because of the rectangular mask used. The diffraction pattern of a rectangular opening consists of a central spot, the shape of which is inversely related to the shape of the aperture; that is, more extended along the direction of the shorter side of the rectangle and vice versa. In the crossed pattern, there are sets of successively weaker spots (see appendix for details).

As is evident from the optical Fourier transforms of the electron micrographs of the negatively stained sub-mitochondrial particles, the scattering object appears to be a non-periodic one. The optical Fourier transforms lack any periodic elements which must have been represented on a reciprocal lattice, provided there had been any regular surface lattice or repeating subunit structure in the plane of inner mitochondrial membrane present in SMP. It seems that the lattice of F_1-ATPase molecules is a completely disordered one. From the optical Fourier transforms of the electron micrographs of negatively stained sub-mitochondrial particles, it can be reasonably deduced that there is a lack of any two-dimensional repeating or subunit structure within the plane of inner mitochondrial membrane (in SMP). The optical Fourier transforms of the SMP resemble the optical Fourier transforms of non-periodic objects.

For the sake of comparison the optical Fourier

transform of the electron micrograph (Figure 15b) of a freeze-fractured and etched replica of catalase crystal is shown in Figure 15c. Figure 15a shows a catalase crystal negatively stained with 2% PTA (pH 7.2). For freeze-fracturing and etching the catalase crystals were suspended in water. The optical Fourier transform of the fractured face of catalase shows distinct repetitive details limited to a resolution of 3.2nm. Basic spacings are 16.1nm and 6.5nm. The optical diffraction pattern shows diffraction spots, symmetrically arranged on the reciprocal lattice. In the electron micrograph of the negatively stained catalase crystal, the lattice repeats are 19nm and 7.8nm.

b. Freeze-etch replicas.

The optical Fourier transform of the mask (Figure 16b) representing the arrangement of particles on the convex fracture face (Figure 16a) of SMP, obtained by freeze-fracturing and etching in 20% glycerol, is shown in Figure 16c. It contains information only about the particles of interest and thus the confusion likely to be caused by both the platinum grain and non-uniform appearance of structures as caused by platinum shadow in the electron micrographs of the freeze-fractured (etched) replica has been avoided. The optical Fourier transform of the mask, representing the arrangement of particles on the convex fracture face of SMP, reveals a diffuse ring

extending from about 9-12nm, with an average radius corresponding to 10.5nm. The spatial frequencies fall predominantly between about 9-12nm range. This demonstrates lack of any regular two-dimensional periodic arrangement of particles in the hydrophobic interior of the membrane. Because if there were any regular two-dimensional lattice of the intramembranous particles in the hydrophobic interior of the membrane, the optical Fourier transform should have displayed sharp diffraction spots of ring(s).

DISCUSSION

F_1-ATPase

The negatively stained preparations of SMP distinctly display the presence of typical ~10.0nm F_1-ATPase ("coupling factor F_1") knobs attached by the stalks to the inner mitochondrial membrane (of SMP). These stalks are the correlates of the oligomycin sensitivity conferring proteins. It is reasonable to assume that if these ~10.0nm F_1-ATPase knobs, as visualized by the negative staining, are present and attached to the SMP, the freeze-etching technique would be most suitable for demonstrating the presence of these particles on the surface of SMP. However, in the present study, deep-etched submitochondrial particles were found to be devoid of any membrane-attached particles. The etch-surface of inner mitochondrial membrane in the SMP appears to be smooth. This observation leads to a paradoxical situation. It seems that results of freeze-etch studies are in agreement with Sjöstrand's suggestion that the "knobs" or "lollipop"-like structures are artifacts produced by the negative staining procedure in that the ATPase molecules would "pop out" due to osmotic shock during the specimen drying. But this argument has two problems. First of all, it has been demonstrated that the F_1-ATPase knobs are present even when the osmotic shock is reduced to a mimimum by negative staining in am-

monium molybdate (Muscatello and Horne, 1968; Muscatello and Carafoli, 1969). Though it is known that the negative stain dries before the specimen by the measurement of ^3H_2O concentrations of negatively stained preparations during drying (Johnson and Horne, 1970), the shrinkage artifacts are still a matter of controversy. On the other hand, the phosphotungstic acid is expected to be a "good" stain because the large number of polar atoms on its periphery induce an ordered structure on the adjacent water molecules and leave the structure beyond it undistorted so that the water can evaporate from the stain with little damage to the surface of the specimen. Therefore it seems less likely that the phosphotungstic acid would induce the artifacts in negative staining. Recently, the stalked knobs have been claimed to be visualized in the ultrathin sections of mitochondria and submitochondrial particles, preferably after glutaraldehyde fixation and staining with methanolic uranyl acetate (Telford and Racker, 1973).

However, as compared with packing density of particles in the negatively stained, unfixed preparations of inner mitochondrial membrane which exhibit approximately 3000 particles/μm^2 of the membrane area (Stoeckenius, 1963), packing density of particles in ultrathin sections (Telford and Racker, 1973) is much less (Zingsheim and Plattner, 1976). However when the particle packing density of face views of negatively stained inner mitochondrial membranes following glutaraldehyde fixation (Keyhani, 1972; Stiles and Crane, 1966) is compared with the particle packing

density in the ultrathin sections of the mitochondria and SMP (Telford and Racker, 1973), both are found to be in agreement. Thus the negative staining and thin sectioning data appear to be reconciled. But the freeze-etch data presents the problem in its interpretation. Recently an interesting observation has been made by Beechey and his coworkers (Beechey *et al.*, 1974). These authors have demonstrated that in the submitochondrial particles extracted with the diethyl ether, the typical inner mitochondrial membrane knobs, which are correlated with ATPase activity, fail to show up in negative staining. The vesicles (SMP) appear to be less regular. One would assume that either the inner membrane knobs have been contracted into the membrane or the PTA now cannot penetrate the membrane and reveal the knobs. However, in these diethyl-ether treated SMP, the membrane bound ATPase is still sensitive to aurovertin, an antibiotic that binds to the ATPase molecule itself (that is the inner membrane knobs). Therefore it appears that the diethyl ether extraction has little effect on the ATPase molecule itself. However, diethyl ether extraction causes a loss of the sensitivity of the ATPase activity to oligomycin, venturicidin, DCCD and triethyl tin. It causes relatively little loss of the lipid (14% of the total membrane phosphorus is extracted) and almost no extraction of protein (just 0.05%) from the membrane. It appears that the lipid loss may be responsible for contracting the F_1-ATPase within the lipid environment

and thereby rendering it inaccessible to the negative stain.

Penefsky and Warner (1965) have proposed a structure for the mitochondrial ATPase which consists of 11 subunits each with a molecular weight of approximately 26000 and the entire complex has a molecular weight of 284,000 (estimated by the sedimentation velocity). Forrest and Edelstein (1970) have confirmed this value. However, subsequent examinations of the molecular weights have led to a revised figure of 340,000-384,000 for the enzyme isolated from rat liver, ox heart and *Saccharomyces cerevisiae* mitochondria (Lambeth *et al.*, 1971; Lambeth and Lardy, 1971; Catterall and Pedersen, 1971; Senior and Brooks, 1971; Tzagoloff and Meagher, 1971). Purified preparations of ATPase molecules from these sources show, on negative staining, the subunits arranged in a hexagonal array. The maximum distance across the hexagon is approximately 10nm (Kagawa and Racker, 1966; Schatz *et al.*, 1967; Kopaczyk *et al.*, 1968; Tzagoloff and Meagher, 1971; Pedersen and Catterall, 1973). If the average molecular weight of the subunits is 55,000 and the subunits are spherical, then based on these assumptions it can be calculated that the diameter of the subunits is approximately 5.5nm and a hexagonal array of these subunits would give rise to a structure with the maximum dimensions of 15nm x 5nm (Beechey, 1974). However, this is not in accordance with the sizes measured in the electron micro-

scope. Therefore it seems more likely that the subunits are not spherical. If one assumes that the subunits are ellipsoids with a minor axis of 3.3nm, the length of the major axis is 11.4nm (Beechey, 1974). A hexagonal array of six of these subunits with parallel major axes gives a structure that agrees well with most of the electron microscope images. But this model does not account for at least one and possibly three other subunits which are associated with the six subunits that have been considered here.

Beechey (1974) has presented a diagrammatic summary of the information available on the protein subunit structure of the oligomycin-sensitive ATPase, isolated from *Saccharomyces cerevisiae* (Figure 17). The structure appears to be a hexagon made up of subunits 1 and 2 (diameter 5nm). The subunit 3 (diameter 4.4nm) is thought to be connected to the cylindrical oligomycin sensitivity-conferring protein (5nm long, 3.0nm diameter) in the centre of the hexagon. 8a and 8b (3.0nm diameter) and 9 (2.6nm diameter) are displayed arranged around the oligonycin-sensitivity conferring protein cylinder. Though the calculated dimensions of this model (15nm x 9.4nm) agree well with the measurements on the negatively-stained oligomycin sensitive ATPase (15nm x 10nm), it must be stressed that this model should be viewed with caution. The subunits in this model are assumed to be spherical in shape, which is probably not the case for the ATPase sub-

units (they are most probably ellipsoidal).

Beechey (1974) envisages the above-described complex of subunits to traverse the thickness of the inner mitochondrial membrane and not protrude from the membrane as observed in the negative staining. This model readily explains the absence of any particles on the etched surface (PS) of the submitochondrial particles that correspond with the stalked knobs seen in the negatively-stained preparations of SMP. This model also explains the presence of a membrane bound ATPase in the diethyl ether extracted SMP (Broughall *et al.*, 1973) which in negative staining reveal the absence of typical inner mitochondrial membrane stalked knobs. Perhaps on negative staining the phosphotungstic acid penetrates between the ATPase molecules with the attached oligomycin sensitivity conferring protein and rest of the oligomycin sensitive ATPase complex to extrude the ATPase and oligomycin sensitivity conferring protein molecules (Cunningham *et al.*, 1967; Beechey *et al.*, 1973.

However, the above given explanation has some serious problems. According to a model of the mitochondrial proton pump (the mitochondrial ATPase system) (Figure 18) described by Racker (1976), it contains a minimum of eight polypeptide chains that are requried for function. The biggest component where the energy transformation takes place is the ATPase (F_1). There are two other coupling factors, OSCP, an oligomycin sensitivity confer-

ring protein and another coupling factor, F_6, that are required for the attachment of F_1 to the membrane. F_0 is a hydrophobic protein factor (Kagawa *et al.*, 1973) containing a proteolipid. It is a membranous preparation from mitochondria and confers oligomycin sensitivity to the F_1-ATPase and is responsible for the transmembranous movement of protons. F_2 is a coupling factor that still needs further characterization (Racker *et al.*, 1970). Though the precise function of F_2 is still unknown, it seems to stimulate the energy coupling by decreasing the permeability of mitochondrial membranes to protons (Racker, 1976). The proteolipid is the most intriguing component of the ATPase system. It is known to interact with energy transfer inhibitors such as DCCD (N,N' dicyclohexyl carbodiimide). The precise molecular correlates of the stalk are also unknown. It could be OSCP or F_6 or both or neither (Racker, 1976). A reasonable alternative is also δ subunit of F_1 which is required for the attachment of the water-soluble ATPase to the membrane (Smith *et al.*, 1975). Presumably the stalk is formed by all three as shown in Figure 18. Racker's model clearly displays the extramembranous location of F_1-ATPase and is in agreement with the results obtained by negative staining of SMP in the present study. Results obtained by thin sectioning of SMP (Telford and Racker, 1973) also support the extramembranous location of F_1-ATPase. Moreover, the reactivity of F_1-ATPase in SMP to nonpermeant diazobenzene is

comparable to that of F_1-ATPase in solution (Schneider *et al.*, 1972) quantitatively. These results would be difficult to reconcile with any model which shows the F_1-ATPase to be submerged in the membrane, and strongly favours the extramembranous location of F_1-ATPase.

There is another line of argument which also favours the extramembranous location of F_1-ATPase. It is known that the negative stains are hydrophilic and hence they should interact with the hydrophilic surfaces only. If the F_1-ATPase was submerged in the lipid milieu of the bilayer in the inner mitochondrial membrane, then it should not be "stained" at all by the PTA in the negative staining. But, since in the negatively stained preparations of SMP the typical "stalked knobs" are clearly seen projecting out from the membrane, it is only reasonable to assume that the F_1-ATPase projects out from the inner mitochondrial membrane and it is not an artifact of negative staining. However this model is unable to explain the smooth appearance of the etched surface of SMP in the freeze-etch experiments done with the SMP suspended in water. More work is clearly needed in this area to unravel the secret of this phenomenon. There may be "non-sublimable" water present on the surface of the SMP and it will render a smooth profile to the etched surface.

In the freeze-fracture of the SMP preparations in 20% glycerol, the typical membrane intercalated particles are observed on both the concave and the convex frac-

ture faces. There is an asymmetry in the distribution of these particles between the two membrane halves. The protoplasmic half has more particles (2000 ± 200 particles/μm^2) in comparison with the exoplasmic half (1300 ± 300 particles/μm^2). These particles most likely represent the components of respiratory chain (Wrigglesworth *et al.*, 1970). A theoretical frequency distribution of the components of the respiratory chain (Klingenberg, 1968) has been calculated from a knowledge of the approximate molecular weights and molar composition of the respiratory chain (Wrigglesworth *et al.*, 1970). Cytochromes would comprise the majority of protein components in such a distribution. Cytochromes fall in the particle size range 4-6nm with a peak at 6nm due to cytochromes a and a_3.

The distribution is given a low frequency tail by the ATPase and various dehydrogenases, between 7-13nm. Assuming a Pt deposition thickness of 1-1.5nm, a particle size distribution has been calculated for the intramembranous particles observed on the fracture faces of the SMP (Figure 11). From this distribution it is obvious that the maximum number of particles belong to 10-12nm range, and it is followed by the particles in the 5-7nm range. Therefore, the freeze-fracture particles do not correspond one-to-one with the members of the respiratory chain (the molecular correlates of the members of the respiratory chain). Some types of associations between the molecules of various members of the respiratory chain would give rise to such

a situation, and it is reasonable to assume so as it would facilitate the cooperative interactions in the respiratory chain.

It is not surprising to find that the particles on the fracture faces are not representative of the individual protein molecules. When membranes reconstituted with rhodopsin are freeze-fractured, despite the low molecular weight of the prosthetic group of rhodopsin (26,500-28,500; Bownds and Gaid-Huguenin, 1970), the fracture faces show ~20nm large particles (Hong and Hubbel, 1972). These particles are too large to represent individual rhodopsin molecules, and therefore it is quite likely that they are multimers. MN-glycoprotein, which is obtained from the erythrocyte membranes (glycophorin, molecular weight ~55,000; Steck, 1974), can be incorporated into liposomes. This protein undergoes multimerization above a critical concentration in the liposomes and shows up as ~8nm large particles in fracture faces, after freeze-fracturing (Grant and McConnell, 1974; Sergrest *et al.*, 1974). Recently Fisher and Stoeckenius (1977) have correlated the freeze-fractured replicas of the purple membrane preparations with the electron density projection worked out by Unwin and Henderson (1975). These authors have determined that each particle in the fracture face contains 9-12 bacteriorhodopsin molecules--63 to 84 transmembrane α-helices.

Optical Diffraction Studies

The results of the optical diffraction experi-

ments on the electron micrographs of negatively stained SMP clearly demonstrate the absence of any subunit structure in the plane of inner-mitochondrial membrane in SMP. Furthermore, it also suggests that the lattice of F_1-ATPase molecules is highly disordered. The data from the optical diffraction experiments on the masks obtained from the electron micrographs of the fracture faces of the SMP also demonstrate a lack of any subunit structure in the hydrophobic interior of the membrane. The intramembranous particles are not arranged in any regular two-dimensional lattice, and the average particle-to-particle distance is 10.5nm. These results negate the presence of the "much discussed" pronounced subunit structure (Green, 1974; Green, 1972; Fernández-Morán *et al.*, 1964) in the plane of the inner mitochondrial membrane. These conclusions are in agreement with the observations of Finean and his co-workers (Thompson *et al.*, 1968) who have studied the inner mitochondrial membrane organization using the technique of small-angle X-ray diffraction. The diffraction patterns obtained from hydrated pellets of the inner mitochondrial membrane (obtained from rat liver mitochondria) showed two or three orders of a lamellar repeat of 11.8nm at water contents of 10-30%. The lameller phase is thought to represent the intact membrane which retains water essential to its integrity. Subsequent alterations in the diffraction patterns on further drying probably represented molecular reorganization within the membrane. These authors

found no X-ray diffraction evidence in support of a pronounced subunit structure within the plane of the inner mitochondrial membrane.

These results, which negate the presence of the subunit or any two-dimensional periodic structure within the plane of the inner mitochondrial membrane, point against the "tripartite repeating unit" (TRU) concept of the inner mitochondrial membrane organization given by Green and his colleagues (Fernandez-Moran *et al.*, 1964; Green and Ji, 1972; Green, 1974). First these authors had invoked the concept of the lipoprotein subunits, which was refuted later on (Stoeckenius and Engelmen, 1968). Now, Green has proposed a model (Green, 1974) in which the mitochondrial supermolecule is envisaged to contain five complexes: the four complexes of the electron transfer chain and a central tripartite repeating unit, which consists of the systems involved in ATP synthesis (the F_1-ATPase) and active transport (the membrane-forming basepiece). But on the basis of the observations made in the present study it seems that there is no repeating unit in the inner mitochondrial membrane.

The concept of the lipoprotein subunits has been abandoned now. In some membranes the presence of a subunit structure (here the word subunit structure refers to the two-dimensional periodic structure within the plane of the membrane as defined in the introduction and therefore it should not be confused with the lipoprotein sub-

units) has been demonstrated. Subunit X-ray diffraction patterns (arising due to the proteins within the plane of the membrane) have been recorded from the disc membranes obtained from the retina, sarcoplasmic reticulum membranes, hepatic gap junctions, purple membranes of the halophilic bacterium *Halobacterium halobium*, and from the quantasomes of the chloroplasts. The subunit diffraction is diffuse and of weak intensity and is therefore not easily recorded. The first X-ray evidence for a subunit structure within the plane of the membrane was obtained from the subunit diffraction pattern recorded from fully hydrated, partially hydrated or air-dried isolated disc membrane preparations (Blasie *et al*, 1965). In the normal hydrated state the lattice of rhodopsin molecules is disordered but in the air-dried disc membranes, rhodopsin molecules are arranged in a square lattice of 7.0 x 7.0nm. In the case of the fully hydrated sarcoplasmic reticulum membranes, a subunit pattern consisting of two diffuse reflections has been recorded. In the normal hydrated state the lattice of ATPase molecules is disordered with an average center-to-center nearest-neighbour distance of about 7.3nm (Worthington and Liu, 1973). Dupont and his coworkers (Dupont *et al.*, 1974) have obtained a subunit pattern from the X-ray study on the membrane fragments from *Torpedo* electric tissue. In the partially dehydrated electroplax membranes, the cholinergic receptor molecules are arranged in a hexagonal array of 9.0nm in size. In the case

of the purple membrane, the unusually regular arrangement of the protein and lipid components was first demonstrated by Blaurock and Stoeckenius (1971). The X-ray diffraction pattern of purple membrane in water consisted of a series of sharp rings, the spacings of which corresponded to a two-dimensional hexagonal crystal with a 6.3nm unit cell. [Recently Unwin and Henderson (Unwin and Henderson, 1975; Henderson and Unwin, 1975) have achieved a notable breakthrough in the analysis of the periodic arrays of biological molecules and they have determined the three-dimensional structure of purple membrane at 0.7nm resolution. The unstained purple membranes in 1% glucose were exposed to very low electron doses, low enough to avoid the destruction of their structure, to obtain the "low dose images". The data obtained from low does images was combined with the data from the electron diffraction patterns. The low dose images were processed to provide the phases (the phases were suitably corrected for the contrast transfer function by utilizing the optical Fourier transforms of the normal high-dose images), and the amplitudes of the structure factors were obtained by measuring the intensities in the electron diffraction patterns. By employing the data obtained for various tilt angles, a three-dimensional Fourier synthesis was computed according to the method given by DeRosier and Klug (1968). The map reveals that the bacteriorhodopsin protein in the membrane is globular and it extends to both sides of the membrane.

It is made up 7 α-helices packed 1.0-1.2nm apart and 3.5-4.0nm in length running perpendicularly to the plane of the membrane. The molecules are arranged around a three-fold axis with a space of 2.0nm in diameter at the centre, which is filled with lipid. The membrane displays a surprisingly great degree of order. Purple membrane is the only example of a biomembrane where we know the structure of a membrane-bound protein *in situ*.] The gap junctions are made up of the units hexagonally arrayed with two-dimensional crystal-like regularity in the plane of the membrane. Goodenough and Stoeckenius (1972) have obtained the subunit reflections from gap junctions corresponding to a hexagonal lattice of 8.6nm.

Very recently Caspar and his group have used X-ray crystallographic methods and electron microscope image analysis to correlate the structure and composition of gap junction plaques isolated from mouse liver (Caspar *et al.*, 1977; Makowski *et al.*, 1977). They have shown that there is a significant short-range disorder in junction lattice, even though the long-range order of array is remarkable. This disorder has provided more information about the nature of forces that hold the array together. In the case of gap junctions and purple membranes, the subunit structure remains unaffected by drying.

It is now known on the basis of the observations of Blasie and Worthington (1969), who had employed the radial distribution functions to analyze the subunit

structure, and that of Poo and Cone (1973), that the rhodopsin molecules in the normal hydrated disc membranes have freedom of motion within the plane of membrane and behave like a "planar liquid". The subunits in the sarcoplasmic reticulum have also been demonstrated to behave in the same way (Worthington, 1976).

What are the probable reasons for the absence of a subunit structure in the plane of the inner mitochondrial membrane? It is known in the case of the cytochrome c that it moves between its oxidase and reductase in the lipid milieu of the membrane (Chance, 1974). For such translational and rotational motions that the cytochrome c undergoes, the membrane lipids must be in a sufficiently fluid state to allow for such motions. And this more fluid lipid environment would reduce the possibility of the organization of membrane proteins in any regular two-dimensional lattice in the plane of the membrane. Most of the membranes which have distinctive subunit structure have a relatively rigid lipid environment. For example in the case of the purple membrane which has a regular subunit structure, the bacteriorhodopsin molecules exist in a very rigid lipid environment (Blaurock and Stoeckenius, 1971). However, there is still a possibility of the existence of regions of high lipid fluidity and relatively rigid lipid environments occurring together in the inner mitochondrial membrane. The evidence for the presence of relatively rigid environments in the inner mitochondrial membrane came from the experi-

ments with cytochrome oxidase, which demonstrated that it is probably completely immobilized in the inner mitochondrial membrane or its rotation is confined to a single axis coinciding with the symmetry axis of heame a_3 (Junge and DeVault, 1975).

The absence of subunit or any two-dimensional periodic structure within the plane of inner mitochondrial membrane indicates that there is, perhaps, a considerable freedom of molecular motion within the plane of the membrane.

However, in relation to the implications of the present work it should be borne in mind that the results reported here are based on the studies of SMP and it is possible that their organization may not be a true represenation of the life-like structure of the inner mitochondrial membrane. This constraint is of particular significance in view of the current concept of the "dynamic" biomembrane organization and function.

PLATES AND FIGURE LEGENDS

Figure 1. A three-dimensional drawing of a triple-layered membrane with a regular subunit structure (Worthington, 1976).

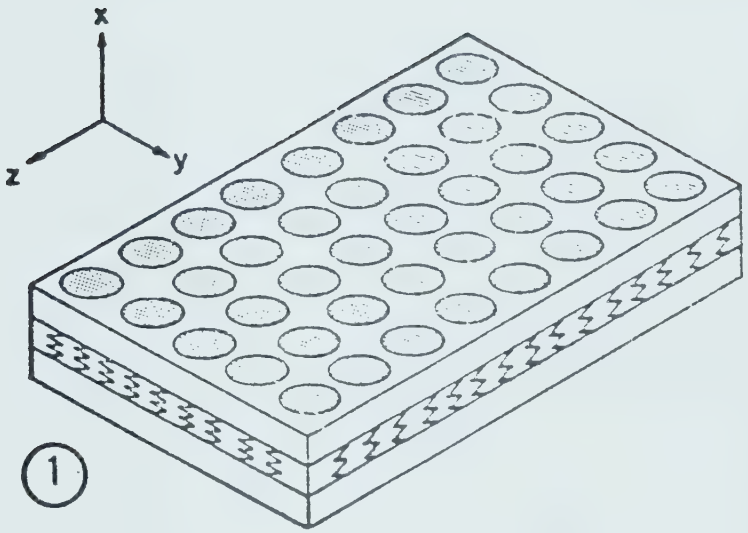
x
z
y
1

Figure 2. Optical diffractometer lens system. Ray diagram showing diffraction and reconstitution positions (Polaron Instruments Inc.).

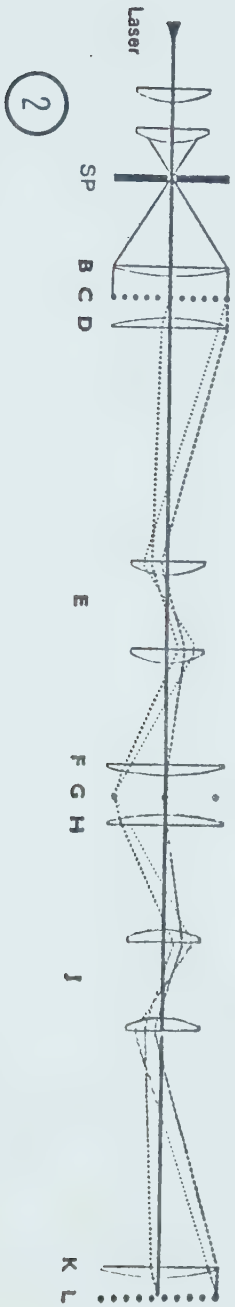
2
Laser
SP
B C D
E
F G H
J
K L

PLATE 1

Figure 3. A typical SMP preparation negatively stained with 2% PTA (pH 7.1). F_1-ATPase knobs are seen attached to the surface of SMP.

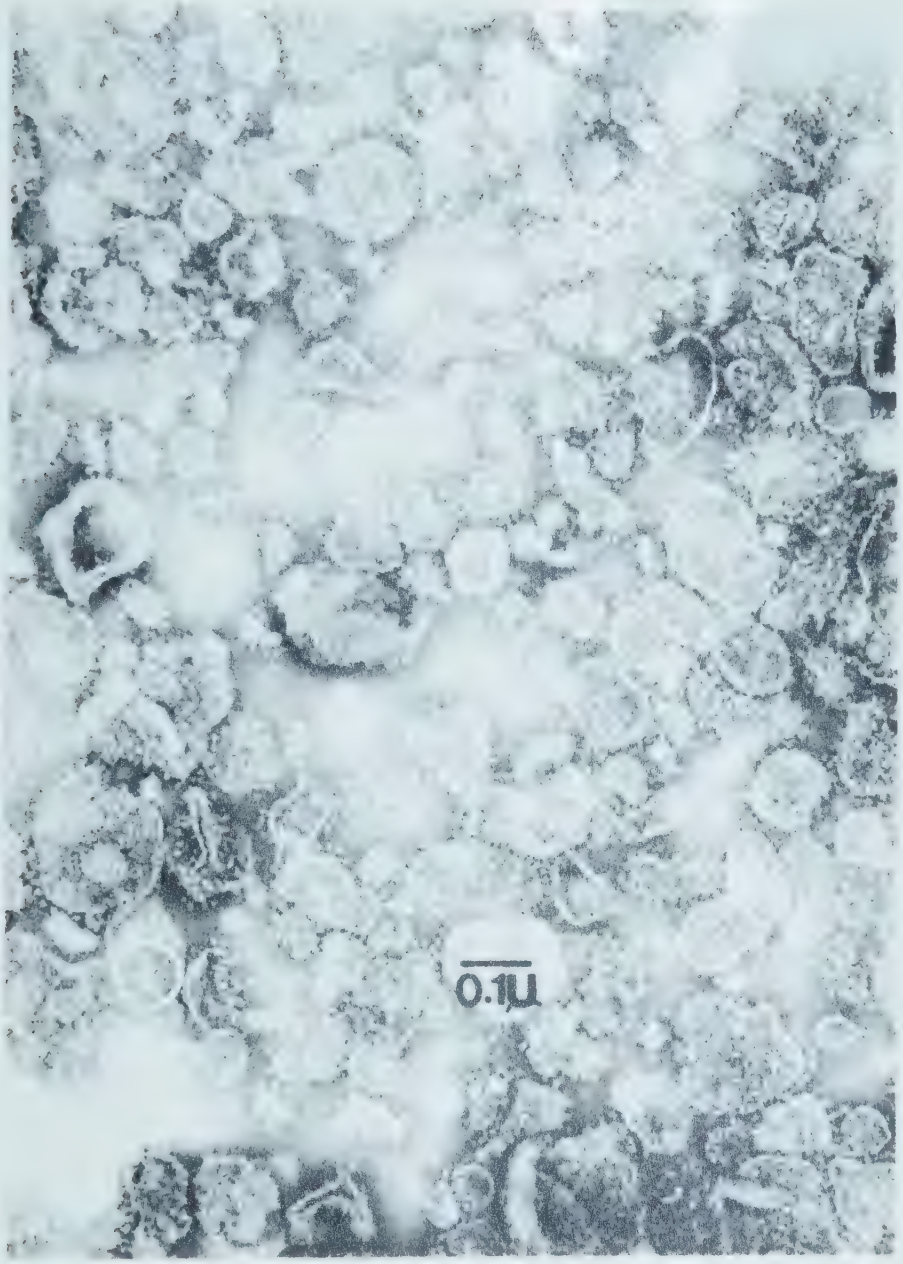
0.1μ

PLATE 2

Figure 4. An SMP preparation negatively stained with 2% PTA (pH 7.a) showing F_1-ATPase knobs attached to the SMP by stalks (arrows point at the stalks).


0.1μ
4

PLATE 3

Figure 5. A negatively stained (with 2% PTA, pH 7.1) "tubularized" preparation of membrane fragments of mitochondrial cristae.

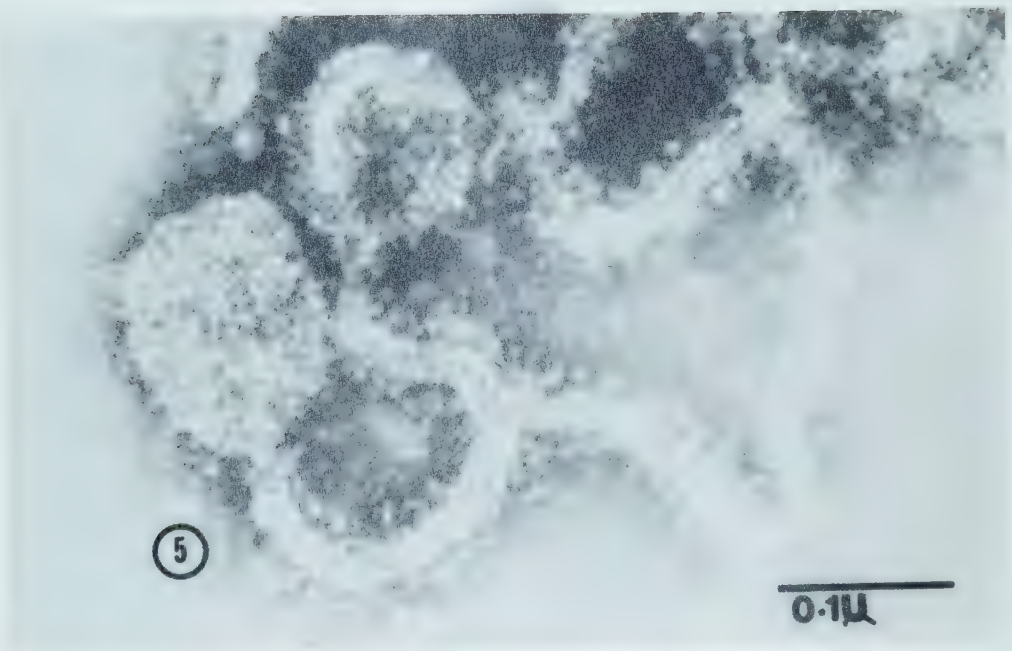
5
0·1μ

Figure 6. Freeze-etch nomenclature for SMP; membranes of mitochondria; freeze-etching of SMP in glycerol; freeze-etching of SMP in water.

C = convex fracture plane
C' = concave fracture plane
EF = exoplasmic fracture face
EH = exoplasmic half
ES = exoplasmic surface
I = inner mitochondrial membrane
O = outer mitochondrial membrane
IMS = the space between the inner and outer mitochondrial membrane
M = matrix
PH = protoplasmic half
PS = protoplasmic surface
PF = protoplasmic fracture face
SP = surface proteins
W = water

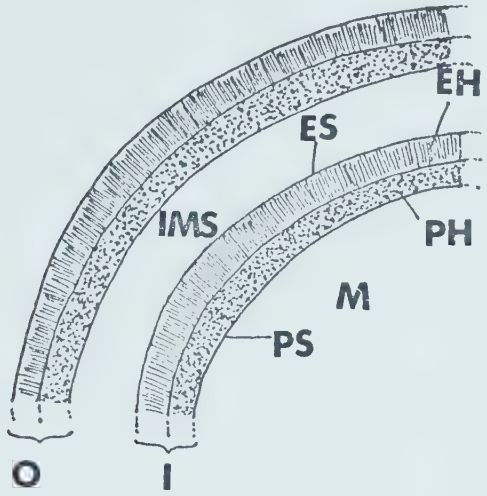

a
MITOCHONDRION

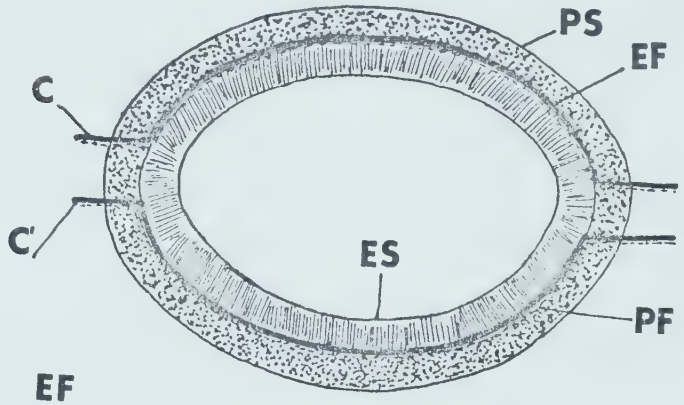

b
SMP IN 20% GLYCEROL

6

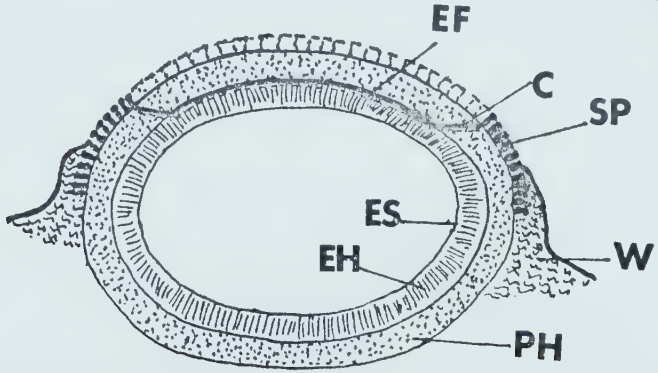

c
SMP IN WATER

PLATE 4

Figure 7. Fracture faces revealed after freeze-etching SMP suspended in 20% glycerol. Arrow indicates the direction of shadowing.

EF = exoplasmic fracture face (convex)
PF = protoplasmic fracture face (concave)

PLATE 5

Figure 8. Typical fracture faces revealed after freeze-etching SMP in 20% glycerol. Arrow indicates the direction of shadowing.


PL
0.1 M

PLATE 6

Figure 9. Typical fracture faces obtained by freeze-etching SMP preparation suspended in 20% glycerol. Arrow indicates the direction of shadowing.


9

PLATE 7

Figure 10. A convex fracture face (EF) revealing the intramembranous particles arranged in irregular rows. Arrows indicate the rows.

Figure 11. Frequency distribution of particle sizes on the SMP fracture faces. Note that most of the particles fall in 10-12nm diameter range. Over 200 particles were counted.

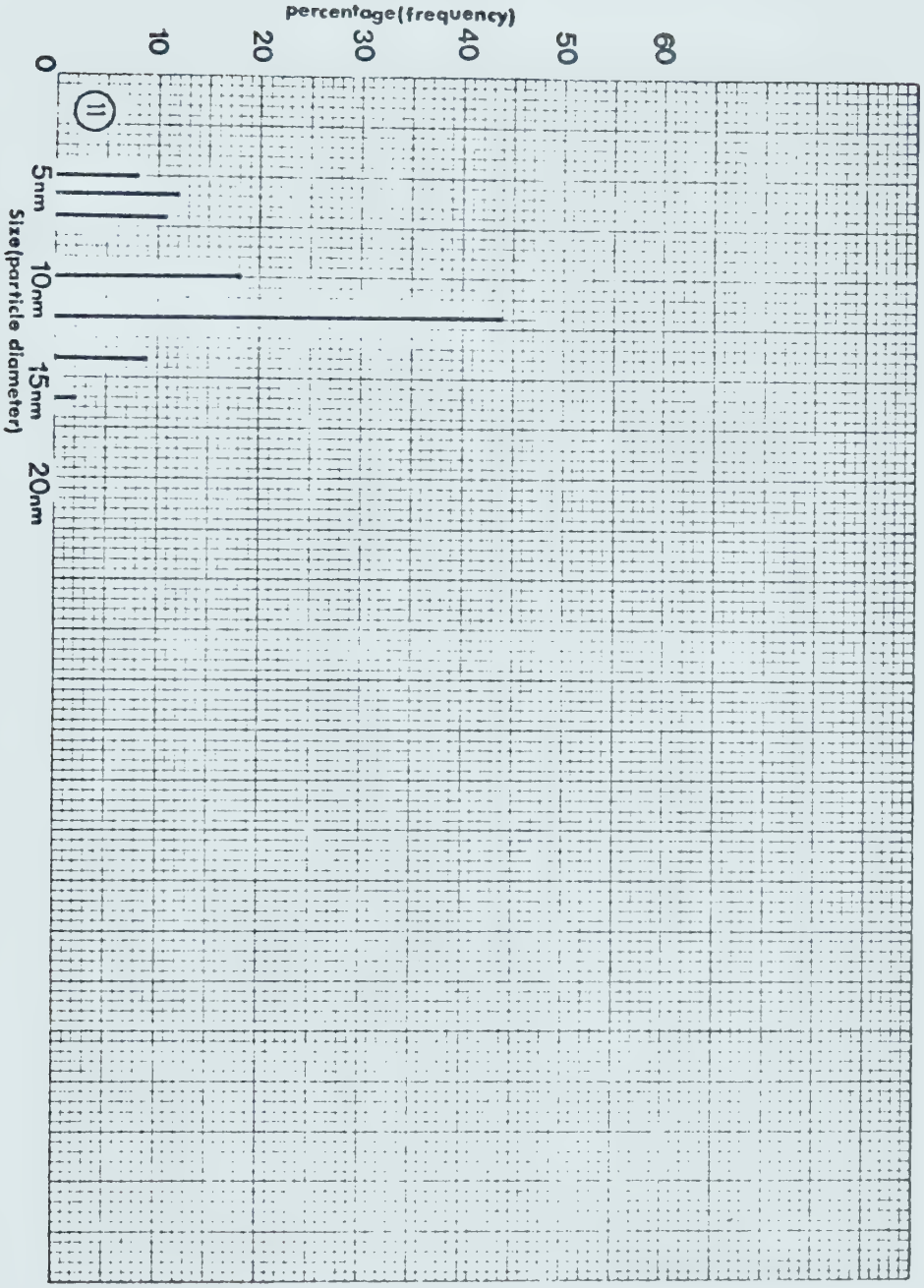
percentage (frequency)
0
10
20
30
40
50
60
(11)
5nm
10nm
15nm
20nm
Size (particle diameter)

PLATE 8

Figure 12. A typical SMP, freeze-etched in water. It displays a rather smooth etched surface (PF) and a typical convex fracture face (EF). Arrow indicates the direction of shadowing.

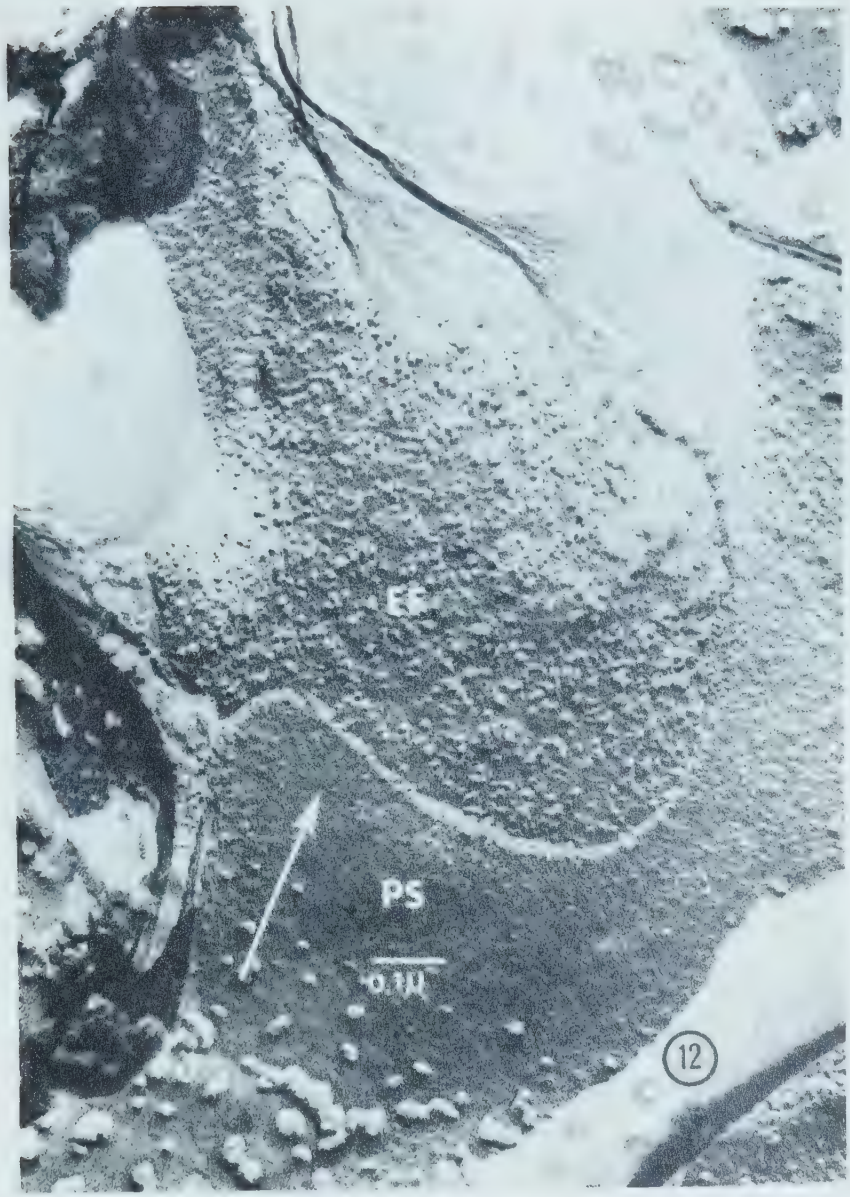
Et
PS
0.1μ
12

PLATE 9

Figure 13a. A typical negatively stained SMP subjected to optical diffraction. The area under the circle was left open and the remainder was masked out in the optical diffraction experiments.

13b. Optical Fourier transform of the area enclosed within the circle in Figure 13a. It reveals an absence of any periodic elements and therefore it eliminates the possibility of a subunit structure within the plane of membrane in SMP.

13b' and 13b". Optical Fourier transform of the same area as shown in Figure 13a, obtained by using shorter exposure times. These, too, reveal an absence of periodic elements.

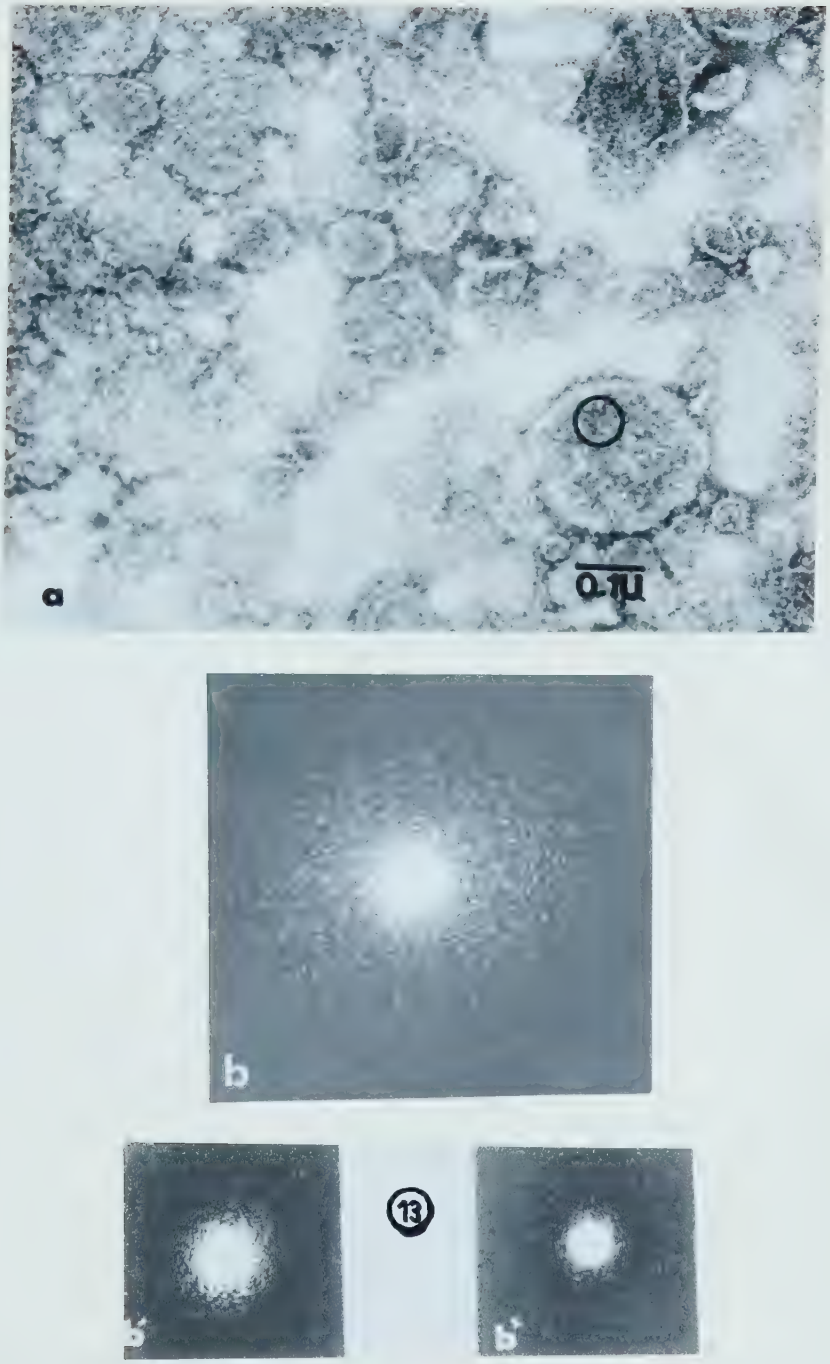
a
0.1μ
b
13
b'
b''

PLATE 10

Figure 14a. An SMP negatively stained with 2% PTA (pH 7.1). The area within the rectangle was subjected to optical diffraction.

14b. Optical Fourier transform obtained from area enclosed within the rectangle in Figure 14a. It reveals an abstinence of periodic elements.

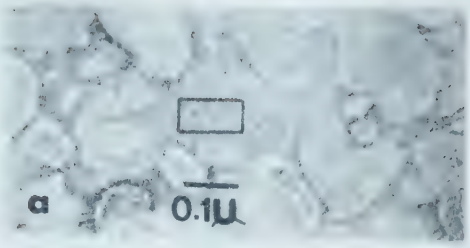

(11)

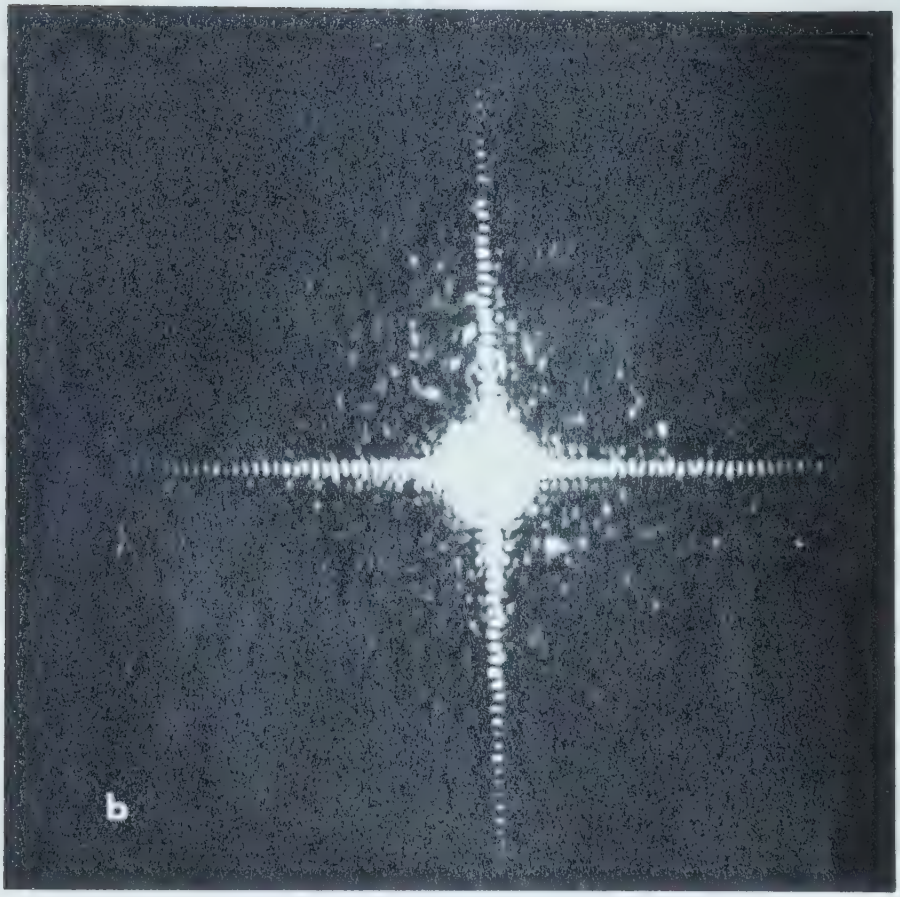

PLATE 11

Figure 15a. A catalase crystal negatively stained with 2% PTA, pH 7.1. The lattice repeats are 19nm and 7.8nm.

15b. A catalase crystal freeze-etched in water. It reveals a fracture face. The area within the rectangle was subjected to optical diffraction.

15c. Optical Fourier transform of the fracture face enclosed within rectangle in Figure 15b. It shows distinctive repetitive details to a resolution of 3.2nm. Basic spacings are 16.1nm and 6.5nm.

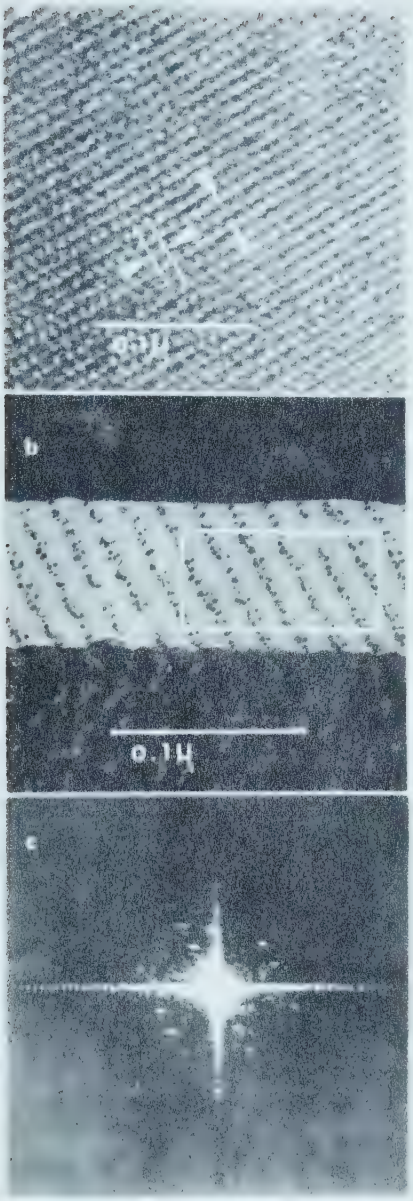

15

PLATE 12

Figure 16a. Convex fracture face (EF) of a freeze-etched SMP. The fracture face displays typical intramembranous particles.

16b. The mask prepared by punching holes at particle positions in the micrograph shown in Figure 16a.

16c. The optical Fourier transform of the mask shown in Figure 16b. The diffraction pattern shows a diffuse ring extending from about 9-12nm, with a mean radius of 10.5nm.

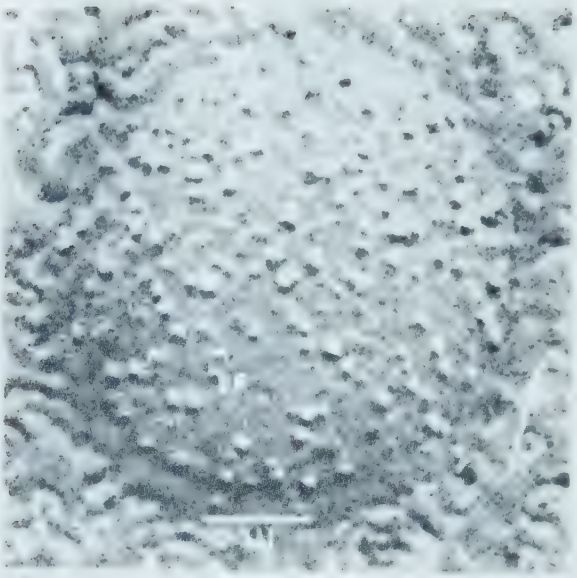

b

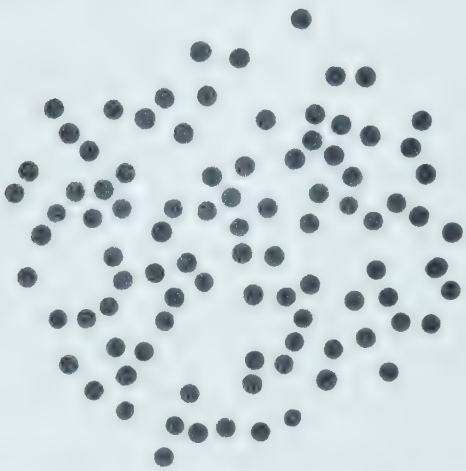

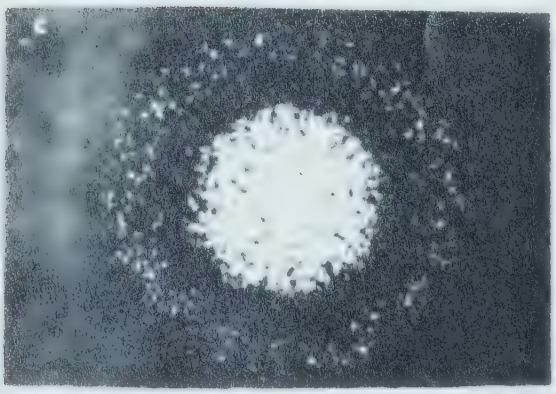

c

Figure 17. Diagrammatic summary of subunit structure of the oligomycin-sensitive ATPase isolated from *Saccharomyces cerevisiae* (Beechey, 1974).

Figure 18. Structure of the mitochondrial proton pump (Racker, 1976). It is intentionally incomplete with respect to the subunit structure of F_1-ATPase, because the topographical positions of the γ and ε subunits (which are deleted in the drawing) are not clearly known.

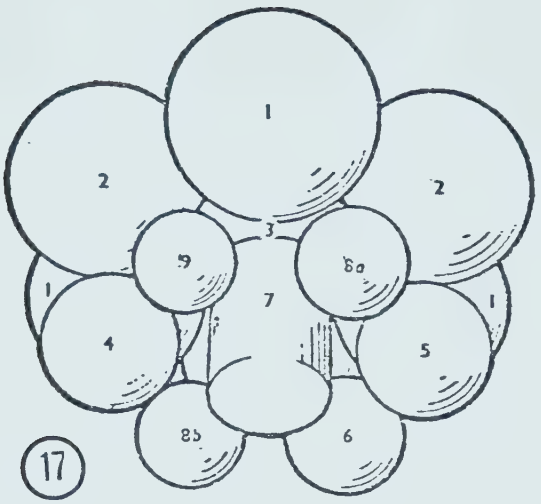
1
2
2
3
1
4
7
5
1
6

17

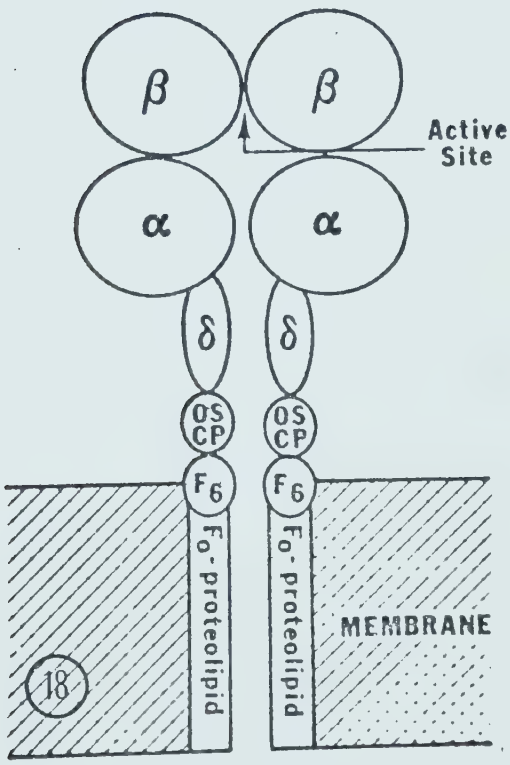
β
β
Active Site
α
α
δ
δ
OS CP
OS CP
F6
F6
Fo - proteolipid
Fo - proteolipid
MEMBRANE

18

Figure 19. Path difference for rays scattered at an angle α from two points A_1 and A_2 (Lipson and Lipson, 1969).

Figure 20. Image formation in a single-lense optical system illuminated with a coherent beam (Johansen, 1975).

Figure 21. Path differences between waves resulting from scattering in a plane object at two object points O and P. The angular coordinates of the interference pattern at point Q are α and β (Johansen, 1975).

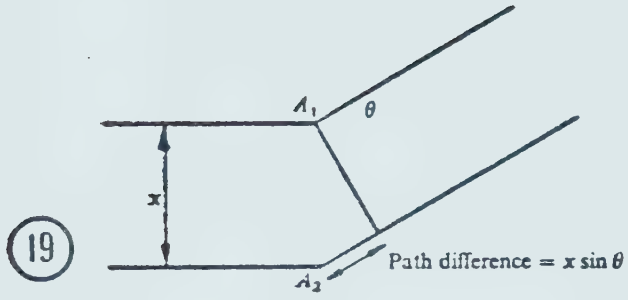
A_1
θ
x
A_2
Path difference = $x \sin \theta$

19

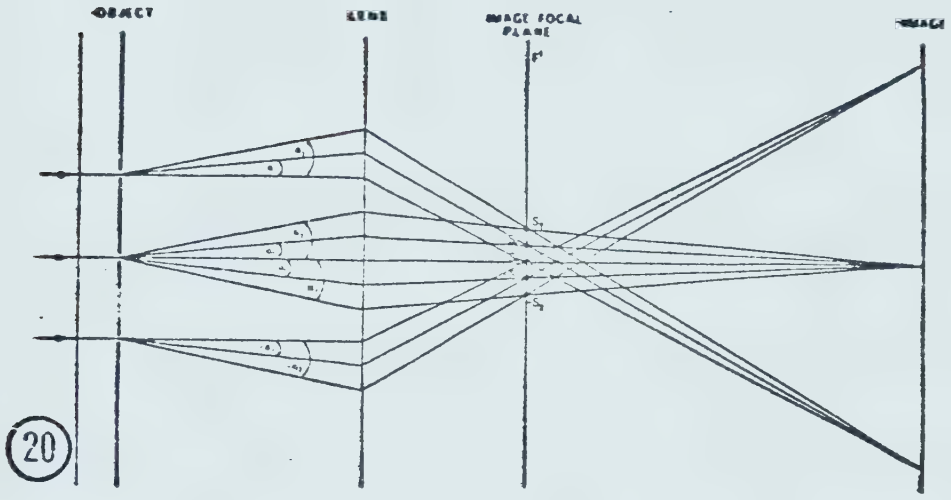
OBJECT
LENS
IMAGE FOCAL PLANE
IMAGE
F'
S_1
S_2

20

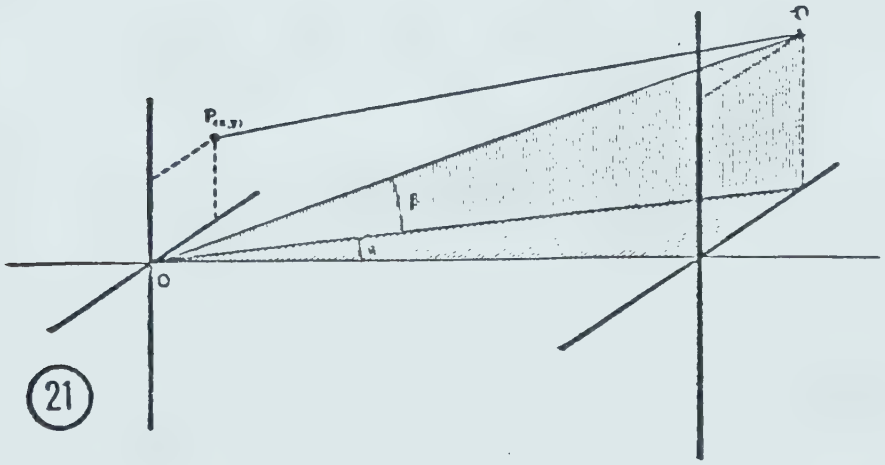
$P_{(x,y)}$
β
α
O

21

BIBLIOGRAPHY

Beechey, R. B. Structural aspects of the mitochondrial membrane-bound adenosine triphosphatase. *Biochemical society special publication*, 1974, *4*, 41.

Beechey, R. B., Lindop, C. R., Broughall, J. M., Griffiths, D. E. and Houghton, R. L. Structural and chemical aspects of the inhibitors of mitochondrial ATP synthesis, in: The mechanism of energy transduction in biological systems (D. E. Green, ed.). *Annals of New York Academy of Science*, 1974, Vol. 227, p. 542.

Beeston, B. E. P. An introduction to Electron Diffraction, in: *Practical methods in Electron Microscopy*, Vol. 1, Part II (A. M. Glauert, ed.). Amsterdam: North-Holland Publishing Company, 1972, p. 195.

Berger, J. E. Optical diffraction studies of crystalline structures in electron micrographs. I. Theoretical considerations. *Journal of Cell Biology*, 1969, *43*, 442.

Berliner, L. J. *Spin labelling: theory and applications*. New York: Academic Press, 1976.

Blasie, J. K., Worthington, C. R. and Dewey, M. M. Molecular localization of frog retinal receptor photopigment by electron microscopy and low-angle X-ray diffraction. *Journal of Molecular Biology*, 1965, *14*, 143.

Blasie, J. K., and Worthington, C. R. Planar liquid-like arrangement of photopigment molecules in frog retinal receptor disc membranes. *Journal of Molecular Biology*, 1969, *39*, 417.

Blaurock, A. E., and Stoeckenius, W. Structure of the purple membrane, *Nature* (London), *New Biology*, 1971, *233*. 152.

Blodgett, K. B. Films built by depositing successive monomolecular layers on a solid surface. *Journal of the American Chemical Society*, 1935, *57*, 1007.

Blundell, T. L. and Johnson, L. N. *Protein Crystallography*. New York: Academic Press, 1976.

Bownds, D. and Gaide-Huguenin, A. C. Rhodopsin content of frog photoreceptor outer segments. *Nature* (London), 1970, *225*, 870.

Branton, D. Fracture faces of frozen membranes. *Proceedings of the National Academy of Sciences (USA)*, 1966, *55*, 1048.

Fracture faces of frozen myelin. *Experimental Cell Research*, 1967, *45*, 703.

Freeze-etching studies of membrane structure. *Philosophical Transactions of the Royal Society of London* (Series B), 1971, *261*, 133.

Branton, D. and Park, R. B. Subunits in chloroplasts lamellae. *Journal of Ultrastructural Research*, 1967, *19*, 283.

Branton, D., Bullivant, S., Gilula, N.B., Karnovsky, M. J., Moor, H., Mühlethaler, K., Northcote, D. H., Packer, L., Satir, B., Satir, P., Speth, V., Staehlin, L. A., Steere, R. L., and Weinstein, R. S. Freeze-etching nomenclature, *Science*, 1975, *190*, 54.

Bretscher, M. S., and Raff, M. C. Mammalian plasma membranes. *Nature* (London), 1975, *258*, 43.

Broughall, J. M., Griffiths, D. E., and Beechey, R. B. Structural aspects of yeast mitochondrial adenosine triphosphatase. *Mechanisms in bioenergetics* (C. F. Azzone, L. Ernster, S. Papa, E. Quagliariello and N. Siliprandi, eds.). New York: Academic Press, 1973, p. 591.

Bullivant, S. Membranes: Freeze-etching techniques applied to biological membranes. *Philosophical Transactions of the Royal Society of London* (B), 1974, *268*, 5.

Caspar, D. L. D., Goodenough, D. A., Makowski, L. and Phillips, W. C. Gap junction structures. I. correlated electron microscopy and X-ray diffraction. *Journal of Cell Biology*, 1977, *74*, 605.

Catterall, W. A. and Pedersen, P. L. Adenosine triphosphatase from rat liver mitochondria I. Purification, homogeneity, and physical properties. *Journal of Biology Chemistry*, 1971, *246*, 4987.

Chalcroft, J. P. and Bulliwant, S. An interpretation of liver cell membrane and junction structure based on osbervation of freeze-fracture replicas of both sides of fracture. *Journal of Cell Biology*, 1970, *47*, 49.

Chance, B. and Montal, M. Ion translocation in energy conserving membrane systems. *Current Topics in Membrane Transport*, 1971, *1*, 99.

Chance, B. The function of Cytochrome C, in The Mechanism of energy transduction in biological systems (D. E. Green, ed.), *Annals of the New York Academy of Science*, 1974, *227*, 613.

Changeux, J. P. and Thiéry, J. On the excitability and cooperativity of biological membranes, in *Regulatory functions of biological membranes* (J. Järnefelt, ed.). Amsterdam: Elsevier Publications, 1968, B.B.A. Library Vol. 11.

Chapman, D. Some recent studies of lipids, lipid-cholesterol and membrane systems. *Biological membranes* (D. Chapman and D. F. H. Wallach, eds.), Vol. 2. New York: Academic Press, 1973, 91.

Cherry, R. J. Protein and lipid mobility in biological and model membranes. *Biological membranes* (D. Chapman and D. F. H. Wallach, eds.), Vol. 3. New York: Academic Press, 1976.

Clark, A. W. and Branton, D. Fracture faces in frozen outer segments from the guinea pig retina. *Z. Zellforsch. Mikrosk. Anat.*, 1968, *91*. 586.

Clayton, R. K. Primary processes in bacterial-photosynthesis. *Annual Review of Biophysics and Bioengineering*, 1973, *2*, 131.

Cooke, R. and Kuntz, I. D. The properties of water in biological systems. *Annual Review of Biophysics and Bioengineering*, 1974, *3*, 95.

Cowley, J. M. *Diffraction physics*. Amsterdam: North-Holland Publishing Co., 1975.

Crowther, R. A., DeRosier, D. J. and Klug, A. Reconstruction of a three-dimensional structure from projection and its application to electron microscopy. *Proceedings of the Royal Society of London* (A), 1970, 317, 319.

Cunningham, W. P., Prezbindowski, K. and Crane, F. L. The relation between structure and function in electron transport systems II. Effect of solvent treatment on membrane strucsure. *Biochimica et Biophysica Acta*, 1967, *135*, 614.

Deamer, D. W. and Branton, D. Fracture planes in an ice-bilayer-model membrane system. *Science*, 1967, *158*, 655.

Deamer, D. W., Leonard, R., Tardieu, A. and Branton, D. Lameller and hexagonal lipid phases visualized by freeze-etching. *Biochimica et Biophysica Acta*, 1970, *219*, 47.

DeRosier, D. J. and Klug, A. Reconstruction of three-dimensional structures from electron micrographs. *Nature* (London), 1968, *217*, 130.

Devaux, P. and McConnell, H. M. Lateral diffusion in spin-labelled phosphatidylcholine multilayers. *Journal of American Chemical Society*, 1972, *94*, 4475.

Dupont, Y., Cohen, J. B. and Changeux, J. P. X-ray diffraction study of membrane fragments rich in acetylcholine receptor protein prepared from the electric organ of Torpedo marmorata, *FEBS Letters*, 1974, *40*, 130.

Erickson, H. P. The Fourier transform of an electron micrograph--First order and second order theory of image formation. *Advances in Optical and Electron Microscopy*, 1973, *5*, 163.

Erickson, H. P. and Klug, A. Measurement and compensation of defocusing and aberrations by Fourier processing of electron micrographs. *Philosophical Transactions of the Royal Society* (London), B, 1971, *261*, 105.

Fernández-Morán, H. Cell-membrane ultrastructure: low-temperature studies of lipoprotein components in lamellar systems. *Circulation*, 1962, *26*, 1039.

Fernández-Morán, H., Oda, T., Blair, P. V. and Green, D. E. The macromolecular repeating unit of mitochondrial structure and function: correlated electron microscopic and biochemical studies of isolated mitochondria and submitochondrial particles of beef heart muscle. *Journal of Cell Biology*, 1962, *22*, 63.

Fessenden-Raden, J. M. Purification and properties of a new coupling factor required for oxidative phosphorylation in silicotungstate treated submitochondrial particles. *Journal of Biological Chemistry*, 1972, *247*, 2351.

Fisher, K. A. and Stoeckenius, W. Freeze-fractured purple membrane particles: protein content. *Science*, 1977, *197*, 4298.

Fleisher, S., Fleisher, B. and Stoeckenius, W. Fine structure of lipid depleted mitochondria. *Journal of Cell Biology*, 1967, *32*, 193.

Forrest, G. and Edelstein, S. J. On the subunit structure of the cold labile adenosine triphosphatase of mitochondria. *Journal of Biological Chemistry*, 1970, *245*, 6468.

Franks, N.P. Structural Analysis of hydrated egg lecithin and cholesterol bilayers, I. X-ray diffraction. *Journal of Molecular Biology*, 1976, *100*, 345.

Frye, L. D. and Edidin, M. The rapid intermixing of cell surface antigens after formation of mouse-human heterokaryons. *Journal of Cell Science*, 1970, *7*, 319.

Glaeser, R. M. Limitations to significant information in biological electron microscopy as a result of radiation damage. *Journal of Ultrastructural Research*, 1971, *36*, 466.

Glaeser, R. M. Radiation damage and biological electron microscopy. *Physical aspects of electron microscopy and microbeam analysis* (B. M. Siegel and D. R. Beaman, eds.) New York: John Wiley and Sons, 1975, 205.

Glaeser, R. M., Cosslett, V. E. and Valdre, U. Low temperature electron microscopy: radiation damage in crystalline biological materials. *Journal of Microscopy*, 1971, *12*, 133.

Goodenough, D. A. and Soeckenius, W. The isolation of mouse hepatocyte gap junctions. *Journal of Cell Biology*, 1972, *54*, 646.

Goodman, J. W. *Introduction to Fourier optics*. New York: McGraw-Hill Book Company, 1968.

Grant, C. W. M. and McConnell, H. M. Glycophorin in lipid bilayers. *Proceedings of the National Academy of Sciences USA*, 1974, *71*, 4653.

Green, D. E. A framework of principles for the unification of bioenergetics, in: The mechanism of energy transduction in biological systems (D. E. Green, ed.) *Annals of the New York Academy of Sciences*, 1974, *227*, 6.

Green, D. E. Membrane structure in relation to the principle of energy transduction and to the principle underlying the control of membrane function. *The structural basis of membrane function* (Y. Haléfi and L. D. Ohaniance, eds.) New York: Academic Press, 1976, 241.

Green, D. E. and Ji, S. The electromechanochemical model of mitochondrial structure and function. *Bioenergetics*, 1972, *3*, 159.

Griffith, O. H. and Jost, P. C. Lipid spin labels in biological membranes. *Spin labelling--theory and applications* (L. J. Berliner, ed.) New York: Academic Press, 1976, 454.

Grubb, D. T. and Keller, A. Beam induced radiation damage in polymers and its effect on the image formed in electron miscroscope. *Proceedings of 5th European congress on electron microscopy*. London: The Institute of Physics, 1976, 544.

Hagins, W. A. The visual process. *Annual Review of Biophysics and Bioengineering*, 1972, *1*, 131.

Hansen, M. and Smith, A. L. Studies on the mechanism of oxidative phosphorylation VII. preparation of a submitochondrial particle (ETP_H) which is capable of fully coupled oxidative phosphorylation. *Biochimica et Biophysica Acta*, 1964, *81*, 214.

Hatefi, Y. The functional complexes of mitochondrial electron-transfer system. *Comprehensive Biochemistry* (M. Florkin and

E. H. Stotz, eds.) Amsterdam: Elsevier Publications, 1966, *14*, 199.

Hatéfi, Y., Galante, Y. M., Stiggall, D. L. and Ohaniance, L. D. Recent advances on the chemistry of the mitochondrial oxidative phosphorylation system. *The Structural Basis of Membrane Function* (Y. Hatéfi and L. D. Ohaniance, eds.) New York: Academic Press, 1976, 169.

Henderson, R. The purple membrane from *Halobacterium halobium*. *Annual Review of Biophysics and Bioengineering*, 1977, *6*, 87.

Henderson, R. and Unwin, P. N. T. Three-dimensional model of purple membrane obtained by electron miscoscopy. *Nature* (London), 1975, 257, 28.

Hodgkin, A. L. *The conduction of nervous impulse*. England: Liverpool University Press, 1963.

Hong, K. and Hubbell, W. L. Preparation and properties of phospholipid bilayer containing Rhodopsin. *Proceedings of National Academy of Sciences, USA*, 1972, *69*, 2617.

Hoppe, W. and Grill, B. Prospects of three-dimensional high resolution electron microscopy of non-periodic structures. *Ultramicroscopy*, 1977, *2*, 153.

Horne, R. W. and Markham, R. Application of optical diffraction and image reconstruction techniques to electron microscopy. *Practical methods in electron microscopy*, Vol. I, Part II (A. M. Glauert, ed.) Amsterdam: North-Holland Publishing Company, 1973, 327.

Horne, R. W. and Whittaker, V. P. The use of negative staining method for the electron microscopic study of subcellular particles from animal tissues. *Z. Zellforsch. Mikrosk. Anat.*, 1962, *58*, 1.

Inesi, G. Active transport of calcium ion in sarcoplasmic membranes. *Annual Review of Biophysics and Bioengineering*, 1972, *1*, 191.

James, R. and Branton, D. The correlation between the saturation of membrane fatty acids and the presence of membrane fracture faces after osmium fixation. *Biochimica et Biophysica Acta*, 1971, *233*, 504.

Johansen, B. V. Optical diffractometry. *Principles and techniques of electron microscopy* (M. A. Hayat, ed.) New York: Van Nostrand Reinhold Company, 1975, *5*, 114.

Johansen, B. V. High resolution bright field electron microscopy of biological specimens. *Ultramicroscopy*, 1977, *2*, 229.

Johnson, M. W. and Horne, R. W. Some observations on the relative dehydration rates of negative stains and biological objects. *Journal of Microscopy*, 1970, *91*, 197.

Jost, M. Die Ultrastruktur von *oscillatoria rubescens* D.C. *Arch. Mokrobiol.*, 1965, *50*, 211.

Junge, W. and Devault, D. *Lasers in physical chemistry and biology* (C. Troyanowski, ed.) Amsterdam: Elsevier Publishing Co., 1975, p. 31.

Kaback, H. R. Transport studies in bacterial membrane vesicles. *Science*, 1974, *186*, 882.

Kagawa, Y. and Racker, E. Partial resolution of enzymes catalyzing oxidative phosphorylation VIII. Properties of a factor conferring oligomycin sensitivity on mitochondrial adenosine triphosphatase. *Journal of Biological Chemistry*, 1966a, *241*, 2461.

Kagawa, Y. and Racker, E. Partial resolution of enzymes catalyzing oxidative phosphorylation IX. Reconstruction of oligomycin-sensitive adenosine triphosphatase. *Journal of Biological Chemistry*, 1966, *241*, 2467.

Kagawa, Y., Kandrach, A. and Racker, E. Partial resolution of enzymes catalyzing oxidative phosphorylation XXVI. Specificity of phospholipid required for energy transfer reactions. *Journal of Biological Chemistry*, 1973, *248*, 676.

Kanner, B. I., Serrano, R., Kandrach, M. A. and Racker, E. A new coupling factor, F_6. *Biochemical Biophysical Research Communications*, 1977 (in the press).

Kauzman, W. Some factors in the interpretation of protein denaturation. *Advances in Protein Chemistry*, 1959, *14*, 1.

Keilin, D. Cytochrome and intracellular oxidase. *Proceedings of the Royal Society* (London), B, 1930, *106*, 418.

Kennedy, E. P. and Rothman, J. E. Rapid transmembrane movement of newly synthesized phospholipids during membrane assembly. *Proceedings of the National Academy of Sciences, USA*, 1977, *74*, 5: 1821.

Keyhani, E. Effect of glutaraldehyde and osmium on the properties of the mitochondrial membrane. *Proceedings of 5th European congress on electron microscopy* (V. E. Cosslett, ed.) Bristol: The Institute of Physics, London, 1972, 270.

Klingenberg, M. The respiratory chain. *Biological Oxidations* (T. P. Singer, ed.) New York: John Wiley and Sons, 1968, 3.

Klug, A. and Berger, J. E. An optical method for the analysis of periodicities in electron micrographs and some observations on the mechanism of negative staining. *Journal of Molecular Biology*, 1964, *10*, 565.

Klug, A. and DeRosier, D. J. Optical filtering of electron micrographs: Reconstruction of one sided images. *Nature* (London), 1966, *212*, 29.

Kornberg, R. D. and McConnell, H. M. Lateral diffusion of phospholipids in a vesicle membrane. *Proceedings National Academy of Sciences USA*, 1971a, *60*, 2564.

Kornberg, R. D. and McConnell, H. M. Inside-outside transitions of phospholipids in vesicle membranes. *Biochemistry*, 1971b, *10*, 1111.

Lake, J. A. Biological studies. *Optical transforms* (H. Lipson, ed.) New York: Academic Press, 1972, 153.

Lambeth, D. O. and Lardy, H. A. Purification and properties of rat liver mitochondrial adenosine-triphosphatase. *European Journal of Biochemistry*, 1971, *22*, 355.

Langmuir, E. The constitution and fundamental properties of solids and liquids. II. Liquids. *Journal of the American Chemical Society*, 1917, *39*, 1848.

Langmuir, I. Pilgrim trust lecture, molecular layers. *Proceedings of the Royal Society (London)*, A, 1939, *170*, 1.

Lee, A. G. Functional properties of biological membranes: A physical-chemical approach. *Progress in Biophysics and Molecular Biology*, 1975, *29*, 1:3.

Lee, A. G., Birdsall, N. J. M., and Metcalfe, J. C. Nuclear magnetic relaxation and biological membrane. *Methods in Membrane Biology* (E. D. Korn, ed.) New York: Plenum Press, 1974, *2*, 1.

Lehninger, A. L. Linked-transport and binding functions in the mitochondrial membrane. *Functional linkage in biomolecular systems* (F. O. Schmitt, D. M. Schneider and D. M. Crothers, eds.) New York: Academic Press, 1975, 165.

Levine, Y. K. Physical studies of membrane structure. *Progress in Biophysics and Molecular Biology* (J. A. V. Butler and D. Noble, eds.) Oxford: Permon Press, 1972, *24*, 1.

Levine, Y. K. X-ray diffraction studies of membranes. *Progress in Surface Science* (S. G. Davison, ed.) Oxford: Pergmon Press, 1973, *3*.

Liktenstein, G. E. *Spin labelling methods in molecular biology.* New York: John Wiley and Sons, 1976.

Lipson, S. G. and Lipson, H. *Optical physics.* London, Cambridge University Press, 1969.

Lipson, H. Basic principles. *Optical transforms* (H. Lipson, ed.) New York: Academic Press, 1972, 1.

Lowry, O. H., Rosebrough, N. J., Farr, A. L. and Randall, R. J. Protein measurement with the Folin-phenol reagent. *Journal of Biological Chemistry*, 1951, *193*, 265.

Luzzati, V. X-ray diffraction studies with lipid-water systems. *Biological membranes* (D. Chapman, ed.) New York: Academic Press, 1968, 71.

Luzzati, V., Tardieu, A., Mateu, L. and Stuhrman, H. B. Structure of human serum lipoproteins in solution. I. Theory and technique of an X-ray scattering approach using solvents of variable density. *Journal of Molecular Biology*, 1976, *101*, 115.

MacLennan, D. H. and Tzagoloff, A. Studies on the mitochondrial adenosine triphosphatase characterization of oligomycin sensitivity conferring protein. *Biochemistry*, 1968, *7*, 1603.

Makowski, L., Caspar, D. L. D., Phillips, W. C. and Goodenough, D. A. Gap junction structures. II. Analysis of X-ray diffraction data. *Journal of Cell Biology*, 1977, *74*, 629.

Malhotra, S. K. and Eakin, R. T. A study of mitochondrial membranes in relation to elementary particles. *Journal of Cell Science*, 1967, *2*, 205.

Malhotra, S. K. Organization and biogenesis of cellular membranes. *Membranes and ion transport* (E. E. Bittar, ed.) London: Wiley Interscience, 1970, *1*, 1.

Malhotra, S. K. On the structure of membranes of mitochondria. *Subcellular Biochemistry*, 1972, *1*, 171.

Malhotra, S. K. and Tewari, J. P. Molecular alterations in the plasma membranes of sporangiophores of *Phycomycae* related to germination. *Proceedings of the Royal Society of London* (B), 1973, *184*, 207.

McConnell, H. M. Molecular motion in biological membranes. *Spin labelling--theory and applications* (L. J. Berliner, ed.) New York: Academic Press, 1976, 525.

Melchoir, D. L. and Steim, J. M. Thermotropic transitions in biomembranes. *Annual Review of Biophysics and Bioengineering*. California: Annual Reviews Inc., 1976, *5*, 205.

Mitchell, P. Chemiosmotic coupling in oxidative and photosynthetic phosphorylation. *Biological Review*, 1966, *41*, 445.

Mitchell, P. Chemiosmotic coupling and energy transduction. *Theoretical and experimental biophysics* (A. Cole, ed.) New York: Marcel Dekker, 1969, *2*, 159.

Mitchell, P. Reversible coupling between transport and chemical reactions. *Membranes and ion transport* (E. E. Bittar, ed.) London: Wiley Interscience, 1970, *1*, 192.

Mitchell, P. A commentary on alternative hypotheses of protonic coupling in the membrane systems catalyzing oxidative and photosynthetic phosphorylation. *FEBS Letters*, 1977, *78*, 1: 1.

Montal, M. Experimental membranes and mechanisms of bioenergy transductions. *Annual Review of Biophysics and Bioengineering*, 1976, *5*, 119.

Mueller, P. and Rudin, D. O. Translocators in biomolecular lipid membranes: their role in dissipative and conservative bioenergy transductions. *Current Topics in Bioenergetics*, 1969, *3*, 157.

Muscatello, U. and Carafoli, E. The oxidation of exogenous and endogenous cytochrome C in mitochondria. A ciobhemical and ultrastructural study. *Journal of Cell Biology*, 1969, *40*, 602.

Muscatello, U. and Horne, R. W. Effect of the toxicity of some negative staining solutions on the elementary structure of membrane-bounded systems. *Journal of Ultrastructural Research*, 1968, *25*, 73.

Oleszko, S. and Moudrianakis, E. N. The visualization of the photosynthetic coupling factors in embedded spinach chloroplasts. *Journal of Cell Biology*, 1974, *63*, 936.

Park, R. B. and Branton, D. Freeze-etching of chloroplasts from glutaraldehyde fixed leaves, *Brookhaven Symposia of Biology*, 1966, *19*, 341.

Parsons, D. F. Mitochondrial structure: two types of subunits on negatively stained mitochondrial membranes. *Science*, 1963, *140*, 985.

Pedersen, P. L. and Catterall, W. A. On the mitochondrial adenosine triphosphatase. *International Congress on Biochemistry, 9th Abstract*, 1973, *4*, Sc.2.

Penefsky, H. A. and Warner, R. C. Partial resolution of the enzymes catalyzing oxidative phosphorylation. VI. Studies on the mechanism of cold-inactivation of mitochondrial adenosine triphosphatase. *Journal of Biological Chemistry*, 1965, *240*, 4694.

Pinto deSilva, P. and Branton, D. Membrane splitting in freeze-etching. *Journal of Cell Biology*, 1970, *45*, 590.

Poo, M. M. and Cone, R. A. Lateral diffusion of rhodopsin in *Necturus* rods. *Experimental Eye Research*, 1973, *17*, 503.

Pullman, M. E., Penefsky, H. S., Dalta, A. and Racker, E. Partial resolution of the enzymes catalyzing oxidative phosphorylation. I. Purification and properties of soluble, dinitrophenol stimulated adenosine triphosphatase. *Journal of Biological Chemistry*, 1960, *235*, 3322.

Racker, E. *Membranes of mitochondria and chloroplasts*. New York: Van Nostrand Reinhold, 1970.

Function and structure of inner membrane of mitochondria and chloroplasts. *Membranes of mitochondria and chloroplasts* (E. Racker, ed.) New York: Van Nostrand Reinhold Company, 1970, 127.

A new look at the mechanisms in bioenergetics. New York: Academic Press, 1976.

Structure and function of ATP-driven ion pumps. *Trends in Biochemical Sciences*, 1976, November, 244.

Racker, E., Tyler, D. D., Estabrook, R. W., Conover, T. E., Parsons, D. F. and Chance, B. Correlations between electron-transport activity, ATP-ase, and morphology of submitochondrial particles. *Oxidases and related systems* (T. E. King, H. S. Mason, and M. Morrison, eds.) New York: John Wiley and Sons, 1965, *2*, 1077.

Racker, E., Fessenden-Raden, J. M., Kandrach. M. A., Lam, K. W. and Sanadi, D. R. Identity of coupling factor 2 and factor B. *Biochemical Biophysical Research Communications*, 1970, *41*, 1474.

Radda, G. K. Flourescent probes in membrane studies. *Methods in membrane biology* (E. D. Korn, ed.) New York: Plenum Press, 1975, *4*, 97.

Rang, H. P. Acetylcholine receptor. *Quarterly Review of Biophysics*, 1974, *7*, 283.

Reimer, L. Review of the radiation damage problem of organic specimens in electron microscopy. *Physical aspects of electron microscopy and microbeam analysis* (B. M. Siegel and D. R. Beaman, eds.) New York: John Wiley and Sons, 1975, 231.

Rose, A. Television pickup tubes and problem of noise. *Advances in electronics*, 1948, *1*, 131.

Scandella, C. J., Devaux, P. and McConnell, H. M. Rapid lateral diffusion of phospholipids in rabbit sarcoplasmic reticulum. *Proceedings of National Academy of Sciences USA*, 1972, *69*, 2056.

Schneider, D. L., Kagawa, Y. and Racker, E. Chemical modification of the inner mitochondrial membrane. *Journal of Biological Chemistry*, 1972, *247*, 4074.

Scheidler, P. J. and Steim, J. M. Differential scanning calorimetry of biological membranes: Instrumentation. *Methods in membrane biology* (E. D. Korn, ed.) New York: Plenum Press, 1972, *4*, 77.

Seelig, J. Anisotropic motion in liquid crystalline structures. *Spin labelling: theory and applications* (L. J. Berliner, ed.) New York: Academic Press, 1976, 373.

Senior, A. E. and Brooks, J. C. The subunit composition of the mitochoncrial oligomycin-insensitive ATPase. *FEBS Letters*, 1971, *17*, 327.

Sergrest, J. P., Gulik-Krzywicki, T. and Sardet, C. Association of the membrane-penetrating polypeptide segment of the human erythrocyte MN-glycoprotein with phospholipid bilayers. I. Formation of freeze-etch intramembranous particles. *Proceedings of National Academy of Sciences USA*, 1974, *71*, 3294.

Sherwood, D. *Crystals, X-rays and proteins*. London: Longman Group Limited, 1976.

Shipley, G. G. Recent-X-ray diffraction studies of biological membranes and membrane components. *Biological Membranes* (D. Chapman and D. F. H. Wallach, eds.) New York: Academic Press, 1973, *2*.

Singer, S. J. The molecular organization of biological membranes. *Structure and function of biological membranes* (L. I. Rothfield, ed.) New York: Academic Press, 1971, 145.

Singer, S. J. and Nicolson, G. L. The fluid mosaic model of the structure of cell membranes. *Science*, 1972, *175*, 720.

Sjöstrand, F. S. Ultrastructure and function of cellular membranes. *The membranes* (A. J. Dalton and F. Haguenau, eds.) New York: Academic Press, 1968, 151.

Sjöstrand, F. S. and Barajas, L. Effect of modifications in conformation of protein molecules on structure of mitochondrial membranes. *Journal of Ultrastructural Research*, 1968, *25*, 121.

Skou, J. C. The ($Na^+ + K^+$) activated enzyme system and its relationship to transport of sodium and potassium. *Quarterly Review of Biophysics*, 1975, *7*, 401.

Slater, E. C. Energy transduction in membranes. *The structural basis of membrane function* (Y. Hatéfi and L. D. Ohaniance, eds.) New York: Academic Press, 1976, 169.

The coupling between energy yielding and energy utilizing reactions in mitochondria. *Quarterly Review of Biophysics*, 1971, *V*, 1.

Sleytr, U. V. Die Gefrierätzung korrespondierender bruchhälflen: ein neur weg xur aufklärung von membranstrukturen. *Protoplasma*, 1970, *70*, 101.

Smith, I. C. P. and Butler, K. W. Oriented lipid systems as model membranes. *Spin labelling: theory and applications* (L. J. Berliner, ed.) New York: Academic Press, 1976, 525.

Smith, A. L. Preparation of beef heart mitochondria: small scale method. *Methods in Enzymology*, 1967, *10*, 81.

Staehlin, L. A. The interpretation of freeze-etched artificial and biological membranes. *Journal of Ultrastructural Research*, 1968, *22*, 326.

Steck, T. L. The organization of proteins in human red blood cell membrane. A review. *Journal of Cell Biology*, 1974, *62*, 1.

Stenn, K. and Bahr, G. F. Specimen damage caused by the beam of the transmission electron microscope. A correlative reconsideration. *Journal of Ultrastructural Research*, 1970, *31*, 526.

Sternlieb, I. and Berger, J. E. Optical diffraction studies of crystalline structures in electron micrographs. II. Crystalline inclusions in mitochondria of human hepatocytes. *Journal of Cell Biology*, 1969, *43*, 448.

Stiles, J. W. and Crane, F. L. The demonstration of the elementary particles of mitochondrial membrane fixed with glutaraldehyde. *Biochimica et Biophysica Acta*, 1966, *126*, 179.

Stoeckenius, W. Some observations on negatively stained mitochondria. *Journal of Cell Biology*, 1963, *17*, 443.

Stoeckenius, W. and Engleman, D. M. Current models for the structure of biological membranes. *Journal of Cell Biology*. 1969, *42*, 613.

Sturtevant, J. M. Some applications of calorimetry in biochemistry and biology. *Annual Review of Biophysics and Bioengineering*, 1974, *3*, 35.

Tardieu, A., Matieu, L., Sardet, C., Weiss, B., Luzzati, V., Aggerbeck, L. and Scanu, A. M. Structure of human serum lipoproteins in solucion. II. Small angle X-ray scattering study of HDL_3 and LDL. *Journal of Molecular Biology*, 1976, *101*, 129.

Telford, J. N. and Racker, E. A method for increasing contrast of mitochondrial inner membrane spheres in thin sections of epon embedded tissue. *Journal of Cell Biology*, 1973, *57*, 580.

Tewari, J. P. Malhotra, S. K. and Tu, J. C. A study of structure of mitochondrial membranes by freeze-etch and freeze-fracture techniques. *Cytobios*, 1971, *4*, 97.

Thompson, J. E., Coleman, R. and Finean, J. B. Comparative X-ray diffraction and electron microscope studies of isolated mitochondrial membranes. *Biochimica et Biophysica Acta*, 1968, *150*, 405.

Tillack, T. W. and Marchesi, V. I. Demonstration of the outer surface of freeze-etched red blood cell membranes. *Journal of Cell Biology*, 1970, *45*, 649.

Traüble, H. and Sackmann, E. Studies of the crystalline-liquid crystalline phase transition of lipid model membranes. III. Structure of a steroid-lecithin system below and above the lipid-phase transition. *Journal of the American Chemical Society*, 1972, *94*, 4475.

Trebst, A. Energy conservation in photosynthetic electron transport of chloroplasts. *Annual Review of Plant Physiology*, 1974, *25*, 423.

Tzagoloff, A. and Meagher, P. Assembly of mitochondrial membrane system. V. Properties of a dispersed preparation of the rutamycin-sensitive adenosine triphosphatase of yeast mitochondria. *Journal of Biological Chemistry*, 1971, *246*, 7328.

Unwin, P. N. T. and Henderson, R. Molecular structure determination by electron microscopy of unstained crystalline specimens. *Journal of Molecular Biology*, 1975, *94*, 425.

Valdré, U. and Zichichi, A. *Electron microscopy in material science.* New York: Academic Press, 1971.

Vanderkooi, J. and Martonosi, A. Sarcoplasmic reticulum. XII. The interaction of O-anilino-1-napthalene sulfonate with skeletal muscle microsomes. *Archives of Biochemistry and Biophysics*, 1971, *144*, 87.

Wahl, P., Ksai, M., Changeux, J. P. and Auchet, J. C. A study on the motion of proteins in excitable membrane fragments by nanosecond flourescence polarization spectroscopy. *European Journal of Biochemistry*, 1971, *18*, 332.

Wallach, D. F. H. and Zahler, P. H. Protein conformations in cellular membranes. *Proceedings of the National Academy of Sciences USA*, 1966, *56*, 1552.

Wehrli, E., Mühlethaler, K. and Moor, H. Membrane surface as seen with a double replica method for freeze-fracturing. *Experimental Cell Research*, 1970, *59*, 336.

Worcester, D. L. Neutron beam studies of biological membranes and membrane components. *Biological membranes* (D. Chapman and D. F. H. Wallach, eds.) New York: Academic Press, 1976, *3*, 1.

Worcester, D. L. and Franks, N. P. Structural analysis of hydrated egg lecithin and cholesterol bilayers. II. Neutron diffraction. *Journal of Molecular Biology*, 1976, *100*, 359.

Worthington, C. R. Structure of photoreceptor membranes. *Annual Review of Biophysics and Bioengineering*, 1974, *3*, 53.

X-ray studies on membranes. *The enzymes of biological membranes* (A. Martonosi, ed.) New York: Plenum Press, 1976, *1*, 1.

Worthington, C. R. and Liu, S. C. Structure of sarcoplasmic reticulum membranes at low resolution. *Archives of Biochemistry and Biophysics*, 1973, *157*, 573.

Wrigglesworth, J. M., Packer, L., Branton, D. Organization of mitochondrial structure as revealed by freeze-etching. *Biochimica et Biophysica Acta*, 1970, *205*. 125.

Yakushiji, E. and Okunuki, K. Ueber eine neue cytochrom-komponente und ihre funktion. *Proceedings of the Imperial Academy*, 1940, *16*, 229.

Zernike, F. *La theorie de images optiques.* Paris: CNRS, 1946.

Zingsheim, H. P. and Plattner, H. Electron microscopic methods in membrane biology. *Methods in membrane biology* (E. D. Korn, ed.) New York: Plenum Press, 1976, *7*, 1.

APPENDIX

A. ABBE'S THEORY OF IMAGE FORMATION

B. CONCEPT OF OPTICAL DIFFRACTOMETER

C. ANALYSIS OF PERIODIC SPACINGS AND ORIENTATIONS IN THE ELECTRON MICROGRAPH

A. ABBE'S THEORY OF IMAGE FORMATION

According to the Fourier theory of Fraunhofer diffraction, the Fraunhofer diffraction pattern of an object is the Fourier transform of the object (Lipson and Lipson, 1969). Amplitude and the phase of the radiation at any point in the diffraction pattern are the amplitude and the phase at the corresponding point in the Fourier transform. Suppose a radiation of wavelength λ is scattered by two points A_1 and A_2 (Figure 19) placed at a distance x apart. If the radiation is incident normally to a line separating two points, the phase difference for waves diffracted at an angle α is equal to $(2\Pi x/\lambda)\sin\alpha$, which can be written as $kx\sin\alpha$ too (where $k = 2\Pi/\lambda$). If there is a collection of points A, each scattering an amplitude f(x), the complete wave diffracted in the direction α is given by

$$\Psi = \int_{-\infty}^{\infty} f(x)\exp(-ikx\sin\alpha)\,dx \qquad \ldots (8)$$

(Lipson and Lipson, 1969). Ψ is the Fourier transform of f(x) in terms of the variable $k\sin\alpha$, which is also called as u. This treatment is one dimensional.

According to Zernike (1946) there are two steps of diffraction, in the process of image formation, in an

optical instrument: the incident light wave is first diffracted by the object and the image is formed by a second diffraction process in which diffraction of the diffraction pattern, produced in the back focal plane of the objective lens, takes place.

However in case of the incoherent illumination, waves will be inclined to the object from a variety of angles. If only one such wave inclined at an angle β to the object is considered, the Fourier transform can be written:

$$\Psi(u,\beta) = \int_{-\infty}^{+\infty} f(x)\exp\left\{-ikx(\sin\alpha + \sin\beta)\right\}dx \qquad \ldots (9)$$

(Lipson, 1972). However, unless f(x) is an extraordinarily simple function, the problem becomes extremely complicated to deal with; therefore in order to explain the image formation process a simple case of plane parallel illumination will be used (Johansen, 1975). In order to complete the requirements of forming an image, it is necessary for an optical instrument to recombine all the scattered waves from one point in the object to a single point in the space because of the fact that the object scatters the plane parallel wave. The occurrence of an image point will be determined by whether all the waves arrive in phase. For the sake of clarity and simplicity, the object is taken to be a diffraction grating illuminated by a coherent plane wave as shown in Figure 20. The incident radiation will be

scattered by the object with the maxima of successive orders at the angles . . . $-\alpha_2$, $-\alpha_1$, 0, α_1, α_2 . . . . These rays would be refracted by the lens so that all rays entering a given angle, α_n, will intersect at a point F' in the image focal plane, also known as the back focal plane.

The diffraction pattern of the object is in the back focal plane of the lens, each point $-s_2$, $-s_1$, s_0, s_1, s_2 being a center of coherently reconstructed rays scattered from the object at a given angle. In this plane, intensity of each point would be observed. (The wave Ψ is a complex quantity and has both amplitude and phase. However in the diffraction pattern only intensity can be recorded. Intensity is equal to $|\Psi|^2$ or $\Psi\Psi^*$, where Ψ^* is the complex conjugate of Ψ.) If the rays are allowed to go further from the back focal plane F' to the image plane I, they will recombine to give the image of the object.

To produce an image, the relative phases between the object points and image points must be the same, and as is obvious the phase change between the object and the back focal plane, F' is opposite and equal to the phase change between F' and the image plane. It therefore implies that the phase relation between the back focal plane of the lens and the image is the inverse of that between the image and the focal plane. Therefore, it can be concluded that the image is the inverse Fourier transform of $\Psi(u)$,

$$f'(x) = \int_{-\infty}^{+\infty} \Psi(u) \exp(iku)\, du \qquad \ldots (10)$$

(Lipson, 1972), indicating the inverse nature of the transformation by omitting the minus sign in the exponential.

So far only the objects in one dimension have been considered by the theory, but two-dimensional plane objects perpendicular to the lens system can also be considered easily. According to Lipson (1972), each point in the object is defined by a vector r, direction of the incident beam is defined by a vector s_0 and that of diffracted beam by a vector s. If the diffracting object is represented by the function f(r), the total scattered wave would be:

$$\Psi = \int_{-\infty}^{+\infty} f(r) \exp \frac{2\Pi i |r|}{\lambda} (\cos\alpha - \cos\beta)\, dA \qquad \ldots (11)$$

Here dA is the element of area around point r, and α and β are angles of incidence and scattering respectively. By giving the vectors s and s_0 moduli of $1/\lambda$, equation (11) can be written as:

$$\Psi = \int_{-\infty}^{+\infty} f(r) \exp 2\Pi i (r \cdot S - r \cdot s_0)\, dA \qquad \ldots (12)$$

or

$$\Psi = \int_{-\infty}^{+\infty} f(r) \exp(2\Pi i r \cdot s)\, dA \qquad \ldots (13)$$

where $S = s - s_0$.

This general expression (Lipson and Taylor, 1958; Lipson, 1972) is valid for all angles of incidence. Equation (13) represents the Fourier transform of the object f(r). To define a complete Fourier transform, two quantities, the phase angle and intensity are needed at each image point. Since the diffraction pattern in the back focal plane of the objective lens gives only intensity $|\Psi|^2$, it is referred to as the optical transform.

B. CONCEPT OF OPTICAL DIFFRACTOMETER

It was assumed in the one-dimensional diffraction theory that the beam illuminating the diffracting object was a plane coherent wave, and that the lens was located close to the object. By mounting a collimating lens in front of the diffracting object, this illumination condition can be achieved to a certain approximation in the optical diffractometer. Under these conditions Fraunhofer diffraction is observed, and its theory has been treated in detail by many authors (Sears, 1949; Goodman, 1968; Lipson and Lipson, 1969). Lipson (1972) has provided a simplified view of the theory which considers a plane diffracting object (Figure 2) illuminated by a plane wave travelling perpendicular to it. It is to be determined, then, how the waves from all points (P), having the coordinates (x,y), add together in a parallel plane at a larger distance (ℓ). If it is supposed that point Q is located at such a plane, the coordinates are $\ell\alpha$ and $\ell\beta$, where α and β are the angular coordinates of the line OQ. The path differences OQ-PQ are equal to $2\ell(\alpha x + \beta y)$, where α and β are very small. The diffraction function $\Psi(\alpha,\beta)$, then, can be obtained by using equation (13). In order to determine the diffraction patterns of various objects, this equation can be used. Of special importance is the object of

an opening where f(x) is constant, it is needed to integrate the expression

$$\Psi(\alpha,\beta) = \int \exp\{-ik(\alpha x + \beta y)\}dxdy \quad \ldots (14)$$

over the area of the opening.

When the periodicities present in an electron micrograph are to be analyzed in an optical diffractometer, usually a rectangular mask is applied leaving out the area of the micrograph which is of no interest. Upon illumination this single opening would produce Fraunhofer diffraction pattern with a central spot. Shape of the central spot is inversely related to the shape of the aperture and in the crossed pattern there are sets of successively faint spots. It can also be treated purely analytically, since the two dimensions can be dealt with separately. Assuming that the two sides of the rectangle are a and b, equation (14) will become

$$\Psi(\alpha,\beta) = \int_{-a/2}^{+a/2} \exp(-ik\alpha x)dx \int_{-b/2}^{+b/2} \exp(-ik\beta y)dy \quad \ldots (15)$$

After integration,

$$\Psi(\alpha,\beta) = ab\frac{\mathrm{Sin}\frac{1}{2}k\alpha a}{\frac{1}{2}k\alpha a} \cdot \frac{\mathrm{Sin}\frac{1}{2}k\beta b}{\frac{1}{2}k\beta b} \quad \ldots (16)$$

which represents the intensity distribution and shape of the Fraunhofer diffraction pattern (Lipson and Lipson,

1969). A circular mask can also be used instead of rectangular opening to leave out the parts of the micrograph that are of no interest. Goodman (1968) and Lipson and Lipson (1969) have presented the theory, explaining the Fraunhofer diffraction pattern of a circular opening, expressing it in terms of Bessel functions. The diffraction pattern of a circular hole consists of a central peak, called the Airy disk, surrounded by the successive weaker rings.

C. ANALYSIS OF PERIODIC SPACINGS AND ORIENTATIONS IN THE ELECTRON MICROGRAPH

The periodic spacings and orientations in the electron micrograph are determined by the analysis of the optical diffraction pattern in a way that is precisely similar to the determination of interplanar spacings and orientations in the specimen by the analysis of the electron diffraction pattern (Beeston, 1973; Horne and Markham, 1973). The distance on the optical diffraction pattern between any particular first order diffraction spot and the central spot is inversely related to the periodic spacings between the repeat features of the micrograph, which has been subjected to optical diffraction. The periodic spacing, d, in the electron micrograph and the distance between the associated first order spot in the optical diffraction pattern and the central spot, R, are related by the following equation:

$$Rd = \lambda L \qquad \ldots (17)$$

where λ is the wavelength of the laser light (632.8nm for the helium neon laser) and L is the diffraction camera length. Camera length of the optical diffractometer can be calibrated by a number of suitable test objects (Horne

and Markham, 1973,) for example, negatively stained micro-crystals of catalase, platinum pthalocyanine crystals, etc.